AD-A227 923

CARBONATE MICROFABRICS

SYMPOSIUM AND WORKSHOP

September 30–October 3, 1990

CO-SPONSORED BY

TEXAS A&M UNIVERSITY
COLLEGE STATION, TEXAS 77843

AND

NAVAL OCEANOGRAPHIC AND ATMOSPHERIC RESEARCH LABORATORY
STENNIS SPACE CENTER, MISSISSIPPI 39529-5004

SP 060:361:90

DTIC
ELECTE
OCT 17 1990
S B D

Approved for public release; distribution is unlimited.

CARBONATE MICROFABRICS

SYMPOSIUM AND WORKSHOP

September 30–October 3, 1990

CO-SPONSORED BY

TEXAS A&M UNIVERSITY
COLLEGE STATION, TEXAS 77843

AND

NAVAL OCEANOGRAPHIC AND ATMOSPHERIC RESEARCH LABORATORY
STENNIS SPACE CENTER, MISSISSIPPI 39529-5004

TABLE OF CONTENTS

INTRODUCTION

BACKGROUND

The idea to organize a symposium and workshop on carbonate microfabrics originated as a result of two years work on a joint NOARL-TAMU project during which we attempted to relate laboratory consolidation and permeability of Recent carbonate sediments to the microfabrics of those sediments. One goal of the project was to demonstrate that differences in microfabrics are responsible for the varying behavior of the geotechnical properties of carbonate sediments during consolidation. During the course of the project, problems such as the definitions of the terms grains and matrix, and even the term microfabric, arose. Grains and matrix are separated at 62.5 µm in terrigenous sediments (Folk, 1980). Ginsburg (1956), in his work on the carbonate sediments of South Florida, placed the boundary at 125 µm. Petrographers, using petrographic microscopes, greatly lowered the dividing line. Folk defined micrite at 5 to 15 µm and designated particles larger than that allochems (= grains). Dunham (1962) specified the lower limit for grains to be 20 µm and Carozzi (1989) used 50 µm as the dividing point. Our work with the SEM on Recent carbonates revealed the arbitrary nature of the particle size boundaries between grains and matrix. Carbonate matrix particles are rigid crystalline bodies of various sizes and shapes that react in the same manner as grains when subjected to dynamic stresses. The SEM reveals that grains vary considerably in size and may be smaller than the arbitrarily defined lower particle size, yet the grains are often sufficiently large to be easily distinguished from the matrix. If in sufficient abundance to form a grain supported sediment, they can control permeability by packing arrangement. In addition, the grains will then transmit stresses and shield matrix particles from compaction.

When we began to discuss the possibility of a symposium with other carbonate specialists one of the most asked questions was "What do you mean by the term *microfabric*?". We were completely surprised by the question as we thought everyone knew the difference between the terms fabric and texture. In our paper (Rezak and Lavoie 1990) we defined *fabric* as: 1) grain-to-grain relationships (shapes, orientations, and nature of grain-to-grain contacts), 2) grain-to-matrix relationships (grain supported versus matrix supported), and 3) matrix component particle relationships (shapes, sizes, orientations, and nature of particle-to-particle contacts). *Grain* is defined as a particle significantly larger than the matrix particle size. Particles are said to be grains if there is room for matrix material to fit in the pore space formed by grains in contact. We might simplify the definition of microfabric as follows: "Microfabric is the microscopic geometry and relationships of all the components of a carbonate sediment or rock including such things as primary sediment, diagenetic features, and pore spaces." Texture, on the other hand, is simply the particle size distribution in the sediment. Perhaps definitions of terms should be addressed during the workshops on Wednesday morning. Defining terms would be reason enough to hold a meeting devoted entirely to carbonate microfabrics.

The relationship between microfabrics and the geotechnical properties of sediments started us thinking about the influence of microfabrics on other fields of study such as acoustics, geochemistry, and hydrogeology. We found such a great amount of interest in microfabrics among specialists in those fields that we decided to invite them to participate in the symposium. So, we will have a variety of specialities present both in the audience and among those presenting papers.

The workshops, scheduled on the last morning of the symposium, are a very important part of the meeting and hopefully everyone will participate in them. Their purpose is to: 1) determine where we are in terms of the nature of our present research activity and goals, 2) outline rele-

vant issues, and 3) recommend directions for future research. The wrap-up at 11:00 a.m. will present a resumé of the deliberations of each workshop in a plenary session. It is hoped that the workshops will result in a white paper describing the state-of-the-art and recommending directions of future research.

ACKNOWLEDGEMENTS

The "Carbonate Microfabrics" Symposium and Workshop has been funded and supported by the Department of Oceanography and the College of Geosciences, Texas A&M University, College Station, Texas; the Texas Institute of Oceanography, Galveston, Texas; the Naval Oceanographic and Atmospheric Research Laboratory, Stennis Space Center, Mississippi; and ARCO Oil and Gas Company, Plano, Texas. We are grateful to the following people for ideas and support during the planning stages of this symposium: Dr. Richard Bennett, Dr. Kathleen Fischer, Dr. William Ward, Dr. Aubrey Anderson, Dr. John Morse, Dr. Harry Roberts, Dr. Patrick Domenico, and Dr. Richard Bachman. In addition, we sincerely appreciated the considerable efforts of Mrs. Sandy Drews who organized mailings, tracked responses, edited this program with abstracts booklet, and generally managed the logistics of the symposium.

Accession For
NTIS GRA&I ☑
DTIC TAB ☐
Unannounced ☐
Justification
By
Distribution/
Availability Codes
Dist | Avail and/or Special
A-1

AGENDA

OUTLINE OF TECHNICAL PROGRAM

I. **KEYNOTE ADDRESS** (Dr. R. Bathurst)

II. **MODERN CARBONATE SEDIMENTS** (D. Lavoie)

- A. **Shallow Water** (P. Sandberg and R. Bachman)
  5 papers
- B. **Deep Water** (C. Neumann and R. Bennett)
  7 papers

III. **ANCIENT CARBONATES** (R. Rezak)

- A. **Shallow Burial Diagenetic Microfabrics** (C. Moore and S. Moshier)
  6 papers
- B. **Deep Burial Diagenetic Microfabrics** (R. Loucks and P. Domenico)
  6 papers

IV. **LAGNIAPPE** (R. Rezak)
  2 papers

V. **FUTURE DIRECTIONS AND RECOMMENDATIONS**
  Workshop Forum

VI. **POSTER SESSION**
  9 papers

CARBONATE MICROFABRICS

SYMPOSIUM AND WORKSHOP

SEPTEMBER 30 - OCTOBER 3, 1990

TEXAS A&M UNIVERSITY

THEME: The Relationship of Microfabric to Fundamental Properties and Processes in Carbonates

OBJECTIVES: The objectives of this symposium are (a) to bring people together from different disciplines to focus on microfabric, (b) to define the-state-of-the-art, (c) to scope out the role and importance of microfabric in understanding processes, such as diagenesis, in carbonates, and (d) to develop new perspectives, new techniques, and future research directions.

SPONSORED BY:

Department of Oceanography and College of Geosciences, Texas A&M University, College Station, Texas
Texas Institute of Oceanography, Galveston, Texas
Naval Oceanographic and Atmospheric Research Laboratory, Stennis Space Center, Mississippi

DEVELOPED AND ORGANIZED BY:

Dr. Richard Rezak, Department of Oceanography, Texas A&M University, College Station, Texas
Dr. Dawn Lavoie, Naval Oceanographic and Atmospheric Research Laboratory, Stennis Space Center, Mississippi

Sunday Afternoon, September 30, 1990

2:00 - 6:00		**Registration** -- First Floor Lobby, Rudder Tower
4:30 - 5:30		**Meeting** with co-chairs and authors, Rudder Tower
6:00 - 6:15		Bus pickup from motels to Faculty Club
6:30 - 8:30		**Icebreaker**, Faculty Club
8:45		Bus pickup from Faculty Club to motels

Monday, October 1, 1990

7:30 - 7:45		Bus pickup from motels to Rudder Tower
8:00 - 9:00		**Registration** -- First Floor Lobby, Rudder Tower
8:30 - 8:45		**Welcoming Remarks**, Room 301, Rudder Tower M. Friedman R. Rezak
8:45 - 9:45	I.	KEYNOTE ADDRESS Robin G. C. Bathurst: **The Relationship of Microfabric to Fundamental Properties and Processes in Carbonates**
9:45 - 10:00		Coffee Break
10:00 - 10:05	II.	MODERN SHALLOW WATER CARBONATE SEDIMENTS Session Statement and Objectives (Philip Sandberg and Richard Bachman)
10:05 - 10:35		Terence P. Scoffin: **Microfabrics of Carbonate Muds in Reefs**
10:35 - 11:05		Cindy K. Carney and Mark R. Boardman: **Sedimentary Microfabrics of Ooid Tidal Channels**
11:05 - 11:35		Roger J. Bain and Annabelle Foos: **Carbonate Microfabrics Related to Subaerial Exposure and Paleosol Formation**
11:35 - 12:05		Harold R. Wanless and Lenore P. Tedesco: **Depositional and Early Diagenetic Controls on Fabrics and Porosity of Carbonate Mud Banks**

12:05 - 1:15		Lunch
1:15 - 1:45		Chris Buczynski and Henry S. Chafetz: **Habit of Bacterially Induced Precipitates of Calcium Carbonate: Examples from Laboratory Experiments and Recent Sediments**
1:45 - 1:50	**III.**	<u>MODERN DEEP WATER CARBONATE SEDIMENTS</u> Session Statement and Objectives (A. Conrad Neumann and Richard H. Bennett)
1:50 - 2:20		Harry H. Roberts and Paul Aharon: **Cold-Seep Carbonates of the Louisiana Continental Slope to Basin Floor**
2:20 - 2:50		Niall Slowey and A. Conrad Neumann: **Periplatform Carbonate Oozes in Northwest Providence Channel: Physical Properties, Acoustic Properties and Microfabric**
2:50 - 3:20		R. Jude Wilber and A. Conrad Neumann: **Effect of Early Cementation on Microfabric of Deep Carbonate Slope Sediments: Hardgrounds and Lithoherms, Northern Bahamas**
3:20 - 3:35		Coffee Break
3:35 - 4:05		Iraj Noorany: **Stress Deformation of Carbonate Oozes**
4:05 - 4:25		Frank R. Rack and William R. Bryant: **Microfabric and Physical Properties of Deep-Sea High Latitude Carbonate Oozes**
4:30 - 6:00		**Cash Bar and Poster Session**, Room 410, Rudder Tower

POSTER PAPERS:

1. Robert L. Folk: **Bacterial Bodies and Carbonate Fabrics: Recent to Triassic**

2. Vicki A. Pedone and William J. Meyers: **Partial Replacement of Low-Mg Calcite by Low-Mg Calcite: Multiphase Microfabrics of Blocky Calcite Cements**

3. Carol de Wet and Stephen Moshier: **Unusual Microfabrics and Cements in a Limestone Interbedded with Coal**

4. Stephen Moshier: **Fabric Controls on Microporosity in Skeletons and Matrix in Limestones**

5. Bruce M. Simonson and Kathy Schubel: **Microbial, Oolitic, and Other Microfabrics in 2.5 Billion-Year-Old Platform Dolomite of Western Australia**

6. Dana S. Ulmer and Peter A. Scholle: **Evaporite Replacement with the Mid-Permian (Leonardian-Guadalupian) Park City Formation, Bighorn Basin, Wyoming**

7. Philip W. Choquette: **Microfabrics and Pore-System Development in "Lime-Mud" Shelf Dolomites: Physical Evidence from Limestone-to-Dolomite Transitions**

8. Isabel P. Montañez: **Systematic Changes in Texture, Microstructure and Geochemistry of Dolomites During Stepwise Stabilization in the Burial Environment**

9. Manmohan Mohanti and Srikanta Das: **Microfabric of Travertine-Tufa Carbonates: Examples from Orissa State, India**

6:15 Bus pickup from Rudder Tower to motels

Tuesday, October 2, 1990

8:00 - 8:15 Bus pickup from motels to Rudder Tower

MODERN DEEP WATER CARBONATE SEDIMENTS
(CONTINUED)

8:30 - 9:00 Dawn Lavoie and William R. Bryant: **Permeability Characteristics of Slope and Deep Water Carbonates from a Microfabric Perspective**

9:00 - 9:30 Roy H. Wilkens, J. Urmos, and Leg 130 Scientific Party: **The Nature of Ooze-Chalk-Limestone Transition in Marine Carbonates: Evidence from the Ontong-Java Plateau, ODP Leg 130**

9:30 - 9:35 IV. SHALLOW BURIAL DIAGENETIC MICROFABRICS
Session Statement and Objectives
(Clyde H. Moore and Stephen O. Moshier)

9:35 - 10:05 John A. D. Dickson: **Graphical Modeling as a Tool for Predicting the Microfabric of Cement Aggregates**

10:05 - 10:20 Coffee Break

10:20 - 10:50 Jeanne Paquette, W. Bruce Ward, and Richard J. Reeder: **Compositional Zoning and Crystal Growth Mechanisms in Carbonates: A New Look at Microfabrics Imaged by Cathodoluminescence Microscopy**

10:50 - 11:20		Robert H. Goldstein: **Fluid-Inclusion Petrography: A Technique for Determining Diagenetic Environment**
11:20 - 11:50		W. Bruce Ward and Richard J. Reeder: **The Use of Growth Microfabrics and TEM in Understanding Replacement Processes in Carbonates**
11:50 - 1:15	Lunch	
1:15 - 1:45		Zakaria Lasemi and Philip A. Sandberg: **Microfabrics and Compositions in Microcrystalline Limestones**
1:45 - 2:15		S. L. Dorobek, T. M. Smith, and P. M. Whitsitt: **Microfabrics and Geochemical Trends Associated with Meteoric Alteration of Early, Near-Surface Dolomite**
2:15 - 2:20	V. DEEP BURIAL DIAGENETIC MICROFABRICS Session Statement and Objectives (Robert G. Loucks and Patrick A. Domenico)	
2:20 - 2:50		Alton Brown: **Stylolites, Styloporosity and Stylocement**
2:50 - 3:20		Peter A. Scholle: **Burial Diagenetic Calcites and Porosity Occlusion**
3:20 - 3:35	Coffee Break	
3:35 - 4:05		D. F. Sibley, J. M. Gregg, R. G. Brown, and P. R. Laudon: **Dolomite Crystal Size Distribution in the Burial Environment**
4:05 - 4:35		Julie A. Kupecz: **Recrystallization of Dolomite with Time**
4:35 - 5:05		Peter Ortoleva and Thomas Dewers: **Genesis of Stylolites and Banded Compaction/Cementation Alternations in Argillaceous Carbonates: A Quantitative Pressure Solution Model**
5:05 - 5:35		Ronald K. Stoessell and William C. Ward: **Effects of Sulfate Reduction on Carbonate Dissolution in Mixing Zone Fluids**
5:45	Bus pickup from Rudder Tower to motels	
7:00	Bus pickup from motels to Hilton Hotel	
7:15 - 8:15	Cash Bar, Hilton Hotel	
8:15	Banquet, Hilton Hotel	
10:15	Bus pickup from Hilton to motels	

Wednesday, October 3, 1990

7:30 - 7:45 Bus pickup from motels to Rudder Tower

8:00 **VI.** LAGNIAPPE
(R. Rezak)

8:00 - 8:30 Anna Dombrowski: **Reinterpretation of Upper Ordovician Red River Carbonates, Cedar Creek Anticline, Williston Basin, USA: Calcrete Weathering of a Shark Bay Ancient Analog**

8:30 - 9:00 David C. Kopaska-Merkel and Steven D. Mann: **Classification of Lithified Carbonates Using Ternary Plots of Pore Facies**

9:00 - 12:00 **VII.** FUTURE DIRECTIONS AND RECOMMENDATIONS

9:00 - 11:00 **WORKSHOPS**

1. Modern Shallow Water Sediments - Sandberg/Bachman, Rm 302
2. Modern Deep Water Sediments - Neumann/Bennett, Rm 305AB
3. Shallow Burial Diagenesis - Moore/Moshier, Rm 308
4. Deep Burial Diagenesis - Loucks/Domenico, Rm 404

Session Objectives: Define the state-of-the-art;
Outline relevant issues;
Recommend directions for future research.

In evaluating your session and material presented, such questions as the following should be considered:

- Where are we now?
- What are the questions that still need to be answered?
- Where do we go from here?
- Are new techniques needed to improve interpretation and utilization of microfabric?
- How do we handle data?
- Do we have appropriate data bases?
- How do we interpret data on scales from microfabric to megafabric?
- Sampling techniques?

11:00 - 12:00 **WRAP-UP SESSION**
(R. Rezak and D. Lavoie)

12:30 Bus pickup from Rudder Tower to motels and airport

ABSTRACTS

ORAL PAPERS

The Relationship of Microfabric to Fundamental Properties and Processes in Carbonates

Robin G. C. Bathurst

At the end of World War II specialist guidance from the literature for carbonate research workers was to be found mainly in the works of Sorby, Cullis, Cayeux and Sander. Sorby in his 1879 address had distilled 30 years of experience with the petrographic microscope. He understood the skeletal content of most limestones, the growth of ooids in agitated water, and the role of dissolved aragonite as a source of carbonate for a variety of cements some of which were epitaxial. Neomorphic calcite was identified in calcitized aragonite skeletons. Cullis's 1904 work on the Funafuti cores included much information on skeletal and diagenetic fabric supported by the use of stains. Cayeux in 1935 produced a major detailed overview of the subject and Sander in his 1936 study of the Triassic Lofer facies, with their geopetal fabrics, had demonstrated the value of meticulous observation allied to rigorous argument. Terminology was derived from Sorby, Grabau, Cayeux and Sander. Sedimentary petrology was rarely taught in universities and research in carbonates stagnated.

Progress in the understanding of microfabrics is about to make extraordinary advances, but always allied to a careful analysis of the accompanying wet chemical and isotopic reactions. Petrology and chemistry go hand in hand.

Towards the end of the 1950's research activity showed signs of awakening when Folk introduced much needed precision into the analysis of limestone constituents and Bathurst offered criteria for distinguishing between sparry calcite cement and neomorphic spar as a replacement of carbonate mud. The most advanced and exciting thinking was going on in Shell Development Company, where Dunham, Ginsburg, Murray, Rezak and others were opening up new horizons. Dunham soon gave us an improved textural outlook with his concept of grain-supported versus mud-supported fabric. Ginsburg made us aware of the importance of early Holocene lithification in freshwater aquifers. The overriding importance of the freshwater diagenetic environment in limestone lithification, with Dunham's vadose products, was popularized by a flood of studies based on tiny uplifted limestone islands with peculiar post-Glacial histories. Many hardgrounds were regarded as products of subaerial exposure.

Lithification came to be seen, in the 1960's, by Land and Friedman as a reorganization of primary carbonate sediment as the less stable aragonite and high-magnesian calcite were dissolved and low-magnesian calcite precipitated either as cement or neomorphic spar. Serious study of the accompanying aqueous chemical reactions had started and use was made of the content of Mg^{2+} and Sr^{2+}, and the values of $\delta^{18}O$ and $\delta^{13}C$. The employment of stains for distinguishing crystal zonation, by Evamy, Shearman and Dickson, made possible the study of cement growth.

There remained those who suspected that marine diagenesis had been more important in the past than was generally believed. Illing's work on modern Bahamian shallow water sediments and Pray's research into the Mississippian of New Mexico both pointed towards diagenetic reactions in seawater. Lindstrôm demonstrated the marine origin of Ordovician hardgrounds on Ôland in the Baltic. Sabkhas were discovered off the Trucial coast of the Persian Gulf. The complex diagenetic relationship between carbonates and evaporites began to be revealed. Holocene dolomite was discovered in the Trucial sabkha, in the Coorong playa lakes near Adelaide, on Bonaire off Venezuela, and on Andros Island, Bahamas. The work of Alderman, Deffeyes, Kinsman, Lucia, Shearman, Shinn, Taylor, and von der Borsch was pre-

eminent in the new outlook on dolomite-evaporite reactions. Modern stromatolites, first described by Black from Andros Island, played a major role in sabkha diagenesis. Bromley's study of Cretaceous Chalk hardgrounds and their relation of trace-fossil sequences revealed new vistas, supported by Fischer and Garrison's work on deep oceanic crusts. Bathurst noted the role of boring cyanophytes and micritic marine cementation in the formation of micrite envelopes. The Bermudan algal cup reefs, investigated by Ginsburg, Schroeder and Shinn, showed active cementation with microcrystalline aragonite and high-magnesian calcite. Alexandersson combined Scuba with the scanning electron microscope to provide details of the crystal habits of similar cements in the Mediterranean. SEM was applied also by Loreau, Fabricius and Klingele to the study of crystal fabric in ooids. At the Bermuda conference on cements in 1969, with a report edited by Bricker, cements were divided into marine and fresh-water, each with the possibility of vadose and phreatic characteristics.

In the U.S.A. Sippel and Glover were developing an attachment to the microscope that revealed enhanced textural detail, especially crystal zonation, by the use of cathodoluminescence.

By the end of the 1960's two important groups of European workers were making a major impression, in Germany led by Mûller in Heidelberg and in Italy by D'Argenio in Naples. In the early 1970's, five important books appeared, by Bathurst (1971) on *Carbonate Sediments and their Diagenesis*, by Purser (1973) on *The Persian Gulf*, by Milliman (1974) on *Marine Carbonates*, by Wilson (1975) on *Carbonate Facies in Geologic History*, and by Flûgel (1978) on *Microfacies Analysis of Limestones*.

A development of great importance in the 1970's was the investigation of groundwater hydrology by Back and Hanshaw and its application to the study of freshwater diagenesis. Meyers proposed the concept of cement stratigraphy. Evidence for the exposure of ancient limestone sequences to freshwater aquifers was given additional support by the recognition of the fabrics of caliches (fossil soils) by Esteban, Freytet and Klappa.

Deep burial diagenesis had hitherto received scant attention but under pressure from the petroleum industry a symposium on the subject was held in Tulsa in 1979. The importance of late burial ferroan calcite and ferroan dolomite, commonly vein related, was stressed by Mountjoy and others for the Devonian of western Alberta, by Dickson and Coleman for the Carboniferous Limestone of the U.K., and by Grover and Readforn for the Ordovician of Virginia. Schlanger and Douglas studied burial diagenesis in deep sea oozes. Wanless, and Buxton and Sibley did much to clarify thinking on the effects of pressure-dissolution. In 1983, disturbed by the obviously severe effects of pressure-dissolution on the structures of oil fields, the oil companies active in the United Arab Emirates organized a seminar with leading academic research workers in Abu Dhabi.

Chemistry in the 1980's became more sophisticated as Brand and Veizer applied the theory of element partitioning, especially in cements. Interest was growing in the diagenetic processes active in the first few metres below the sea floor. Thus Berner and Raiswell were studying the growth of microspar in concretions and the role of bacteria in sulphate reduction, fermentation and methanogenesis. Organic carbon signatures in $\delta^{13}C$ were recognized. Einsele and colleagues studied the lithification of sediments in closed chemical systems. Earlier identifications of sparry cements as necessarily of freshwater origin were queried in the light of discoveries of undoubted marine spar. Attention was increasingly paid to that most complex diagenetic environment in which carbonate sediments are buried in their own seawater and never encounter a freshwater aquifer.

Microfabrics of Carbonate Muds in Reefs

Terence P. Scoffin

The interstices of reef frameworks provide significantly different environments for the accumulation and preservation of fine sediments from those found on the inter-reef sea bed, for the following reasons:

- The reef framework provides indigenous sediment.
- The reef framework is isolated by elevation (and to a limited extent by biological filtering) from off-reef (notably clay mineral) sedimentation.
- Once deposited, internal sediments are normally undisturbed by currents and infauna; thus the sedimentary consequences of short-lived events which are likely to be blurred by reworking in off-reef sediment accumulations may be preserved in a fine stratigraphic record within reef cavities.
- Sediments trickling from point sources of supply into protected recesses may pile into pinnacles which are preserved perched on ledges within cavities.
- Cavities are sheltered from overburden pressure by the rigid framework, consequently internal sediments do not show mechanical or chemical compaction fabrics and grains are normally delicately preserved.
- The prominence and rigidity of the reef framework in an environment of high water flux promotes synsedimentary cementation of internal sediments.
- Anaerobic diagenesis may be mediated by framework microbes.

The components of reef-internal sediments are from four sources:

- Off-reef material carried in by suspension e.g. plankton tests, clay minerals. (The supply of such material may be seasonal).
- Reef-surface debris e.g. Halimeda fragments
- Within-reef framework biogenic production e.g. sponge-bored chips, ascidian spicules
- Silt-sized peloids formed by magnesium calcite precipitation in near-sealed framework voids.

Each individual cavity undergoes a history of progressively restricted water circulation as the throats seal. This commonly results in a characteristic sequence of cavity fill.

Sedimentary Microfabrics of Ooid Tidal Channels

Cindy K. Carney and Mark R. Boardman

Tidal channels within ooid sand shoals are involved in the longshore transport of ooids, the offbank transport of ooids and perhaps the generation of ooids. Channels are oriented perpendicular to the axis of highest ooid concentration and are linked to the transport systems by their ebb-tidal deltas.

On Joulters Cays, Bahamas, surface samples and cores from four channels provide information on trends of microfabrics which should be useful for interpretation of ancient oolites. Petrographic characteristics of tidal channel sediments reflect the surrounding environment. The percent ooids is maximum at the ebb-tidal delta and decreases both seaward and bankward where peloids (probably a combination of micritized ooids and fecal pellets) increase in abundance. Bioerosion of ooids (micritization as well as borings within laminae and across laminae) is minimal at the ebb-tidal delta and increases rapidly up channel into more stabilized areas. Ooids are well sorted, small and superficially coated on the ebb-tidal delta; whereas within the channel, ooids are bimodal in size and less well sorted. Nuclei are dominated by peloids. A trend of increasing size of ooids in the direction of longshore transport is apparent. Size variation of ooids is not dependent on the size of the nucleus. Bimodality of ooids probably results from a combination of in place ooid generation and transport under variable energy conditions. Bioerosion of ooids (micritization, boring) occurs during periods of quiescence in portions of the ooid tidal channels.

Tidal channels can migrate, be blocked for variable time periods, and can rapidly fill with sediment. Lime mud within ooid tidal channels is comprised of layers (several cm thick) of creamy, pelleted aragonite with sharp contacts with ooid sands above and below. Lime mud layers within high-energy tidal channels may result from storm transport of lime mud from interior lagoons or from in-situ accumulation during a period of blockage.

Carbonate Microfabrics Related to Subaerial Exposure and Paleosol Formation

Roger J. Bain and Annabelle Foos

Subaerial diagenesis produces a distinct imprint on carbonate sediments which is recognizable in the rock record. Megascopically, paleosols and subaerial exposure surfaces are recognized throughout the Phanerozoic. Evidence for subaerial diagenesis can also be recognized on a microscopic level. In addition to vadose diagenetic features such as cement and porosity, pedogenic processes leave a distinct set of characteristics.

Patchy distribution of cements and porosity are characteristic of vadose diagenesis. Cement types include 1) equigranular blocky low-Mg calcite in the form of meniscus, rims, pendants and pore-filling cements, 2) minor syntaxial overgrowths, and 3) whisker cements. Dissolution of unstable grains results in formation of intragranular to moldic porosity.

Biota play an important role in pedogenic processes. A number of features can be attributed to the presence of plant roots such as root-hair sheaths, Microcodium, alveolar textures, and the development of vuggy porosity. Micritization of primary fabrics results in development of laminar crusts and soil pisolites. Other pedogenic features include fungal and algal borings, blackened pebbles and surfaces, clay skins, fracturing and microfracturing.

Petrographic features observed in modern and Pleistocene subaerial exposure surfaces will be compared with Phanerozoic examples.

Depositional and Early Diagenetic Controls on Fabrics and Porosity of Carbonate Mud Banks

Harold R. Wanless and Lenore P. Tedesco

The fabric, porosity and diagenetic potential of carbonate mud banks appear to be defined by the interaction of depositional and early diagenetic sedimentation processes. Carbonate banks in and on the margins of Florida Bay and Biscayne Bay in southeast Florida contain four depositional facies that each show great textural variation depending on setting (**interior settings** vs *exposed marginal settings*): (1) fining-upwards units (0.1 to 2 m in thickness) of **layered grainstone to mudstone** and *rudstone to grainstone* are the dominant bank building facies; (2) current-baffling and sediment-trapping by seagrass communities generates **wackestones to packstones** and *fine-grained grainstones* in areas not catastrophically smothered or eroded by frequent storms; (3) autochthonous biogenic depositional units of **calcareous algal grainstones** (Halimeda opuntia) **and mudstones** (Acetabularia) and *coralgal rudstones* occur in areas of increased wave and current activity associated with bank shoaling; and (4) sorted grainstones to rudstones represent frequent reworking associated with shallowing to the intertidal zone.

Repetitive excavation of deep open burrow networks and storm infilling of networks (with grainstones and mud-poor packstones) can result in partial to complete transformation of depositional facies and generation of new sediment fabrics, greatly enhanced porosity and permeability, modified sediment composition and a changed diagenetic and dolomitization potential. Burrow transformed facies dominate those portions of banks where the surface is gradually accreting -- the broad interior (core) to most banks. This is a dominating influence on carbonate banks (and level platform bottoms) influenced by more normal marine waters, but the banks associated with the restricted waters of central and inner Florida bay are not significantly transformed.

Habit of Bacterially Induced Precipitates of Calcium Carbonate: Examples from Laboratory Experiments and Recent Sediments

Chris Buczynski and Henry S. Chafetz

Bacteria induce the precipitation of calcium carbonate in the laboratory and in nature by altering the chemistry in their microenvironment. Cultures of aerobic and facultative bacteria from cyanobacterial mats on Andros Island, Bahamas, and Baffin Bay, Texas, induced the precipitation of calcium carbonate under controlled conditions in more than 120 experiments. Crusts, the largest features formed, are composed of 5-200 μm diameter bundles which are, in turn, composed of numerous individual crystals. The smallest observed features are 0.1-0.4 μm spheres and rods which comprise some individual crystals and crystal bundles.

Crystal bundles resembling rhombohedra, tetragonal disphenoids, tetragonal dipyramids, and calcite dumbbells appear to be uniquely bacterial in origin, and they have all been observed in recent sediments. Swollen rods, discs, curved dumbbells, and 50-200 μm optically continuous crystals resembling brushes may be uniquely bacterial in origin, however, they have not been reported by other laboratories nor observed in natural settings. Presence of any of these forms in recent sediments should be taken as strong evidence for bacterial influence. Spheres and aragonite dumbbells have also been observed in natural environments, however, they are not always bacterial in origin.

Cold-Seep Carbonates of the Louisiana Continental Slope to Basin Floor

Harry H. Roberts and Paul Aharon

Research submersibles are being used in a study of massive carbonate buildups on the Louisiana continental slope and adjacent basin floor. Geohazard survey data (high resolution seismic profiles and side-scan sonographs) as well as submersible observations confirm the widespread occurrence of complex seafloor topography associated with highly faulted areas of seafloor commonly overlying and on the flanks of salt diapirs. Direct sampling of these unusual buildups from the shelf edge (134 m) to a depth of approximately 2500 m indicates that they are composed of authigenic carbonate of various mineralogies (aragonite, Mg-calcite, and dolomite). These carbonates are characterized by extreme depletion of the C-13 isotope (to values of 53.9 ‰ PDB) which associates them with carbon from oil and gas (both biogenic and thermogenic). Hydrocarbons are transported to the seafloor via numerous diapir-related faults. Bacterial oxidation of the hydrocarbons and sulphate reduction in the presence of hydrocarbons in anoxic settings creates isotopically light carbon dioxide and bicarbonate in pore waters which promotes carbonate precipitation. Six species of bacteria responsible for these reactions have thus far been identified from active seep areas. Cements range from microcrystalline Mg-calcite and aragonite through botyroidal and acicular aragonites to euhedral dolomite. At this early stage of investigation the aragonites and Mg-calcites appear to be products of surface and near-surface processes while the dolomites seem to be subsurface products based on rock relationships and geochemistry.

Detailed geochemical work on the shelf edge/upper slope carbonates suggests that the conspicuous ^{18}O enrichments observed for both chemical and bioherm carbonates (^{18}O values ranging from 2.8 to 4.2 ‰ PDB) are attributed to sea bed temperature effect (8 to 18°C) superimposed on the ^{18}O composition of the GOM slope waters (0.7 to 1.6 ‰ SMOW). Unlike the bioherm carbonates which yield ^{13}C values typical of the ambient benthic marine environment (-0.2 to 2.9 ‰ PDB), the authigenic carbonates show anomalous ^{13}C-depleted values (-18.5 to -53.9 ‰ PDB). These ^{13}C compositions are interpreted to represent mixed CO_2 sources derived from bacterial oxidation of methane, crude oil biodegradation, and inorganic (sea water) bicarbonate. A biogenic origin for the methane (^{13}C of -69 to -81 ‰ PDB) is inferred on the basis of mass balance estimates from paired $^{13}C/^{14}C$ determinations. The presence of the planktonic foraminifer G. menardii species in the fossil reef bioherms, coupled with preliminary radiocarbon values, place an early Holocene age for the biogenic reefs that cap these seep-related authigenic carbonates at the shelf edge/upper slope environment.

Periplatform Carbonate Oozes in Northwest Providence Channel: Physical Properties, Acoustic Properties and Microfabric

Niall Slowey and A. Conrad Neumann

We have studied the physical and acoustic properties of Quaternary periplatform sediment in a core from Northwest Providence Channel, Bahamas. The following properties were determined: carbonate mineralogy, grain size distribution, water content, porosity, saturated bulk density, the degree of cementation and compressional velocity. Velocity correlates negatively to the aragonite-to-calcite ratio, water content and porosity, while velocity correlates positively to grain size and the observed degree of cementation. Correlation between velocity and saturated bulk density may be weak as a result of hollow foram and pteropod tests. While not volumetrically very significant, changes in cementation affect velocity in a particularly strong way.

Changes in all parameters correlate to Quaternary climate/sea-level fluctuations and affect velocity in complementary fashion such that velocity is higher during glaciations/sea-level lowstands than during interglaciations/highstands. As a result, acoustic reflections on high resolution seismic profiles can correspond to transitions in climate/sea level. To appreciate the role of sediment physical properties and microfabric in controlling sediment acoustic properties, the processes linking changes in sediment physical properties and microfabric to changes in climate and sea level must be understood.

Effect of Early Cementation on Microfabric of Deep Carbonate Slope Sediments: Hardgrounds and Lithoherms, Northern Bahamas

R. Jude Wilber and A. Conrad Neumann

Early cementation of slope sediments in the northern Bahamas results in the widespread occurrence of hardground and lithoherms in the Straits of Florida. Cemented slope ıacies are composed of packstones and muddy grainstones in which the mud is magnesium calcite of authigenic origin. Such deposits may be or juxtaposed with muddy slope units of detrital origin which have a similar high (> 70%) mud content. Differentiating origin of mud on the slope can be made on the basis of mineralogy and microfabric petrography.

Authigenic magnesium calcite exhibits a series of discrete microfabrics arranged in microstratigraphic sequence. The complete sequence consists of a) a basal zone of amorphous, micritic magnesium calcite, b) an intermediate zone of clotted and peloidal precipitates and c) an upper zone of microspar and spar rim cements. The sequence of cements and gradational induration of slope rocks suggests that early-formed precipitates form a porous and paste-like matrix which becomes increasingly rigid as later stage precipitation occludes microporosity.

In rocks from the deepest parts of the slope (> 600 m) authigenic mud content may exceed 80%. Upper slope rocks (< 300 m) generally contain more spar and peloids but may still contain up to 40% mud. The packstone and muddy grainstone texture of the rocks demonstrates that authigenic precipitates were an early void-filling addition to predominantly mud-free sediments.

The characteristic microfabrics of authigenic magnesium calcite may survive early seafloor alteration to calcite and may thus be preserved during burial. Alternatively, transformation of metastable magnesium calcite during burial may result in highly altered diagenetic microfabrics in these same rocks.

Precipitation of magnesium calcite is inhibited by deposition of detrital aragonite mud originating on adjacent bank tops. Aragonitic slope units are rarely cemented and show none of the characteristic microfabrics of the cemented horizons. Rather, aragonite needles form a dense micritic groundmass with low permeability and allochem content. This suggests that the physical sedimentological conditions favorable to the formation of authigenic muddy limestones occur primarily during sea level lowstands when banktop input to the slope is greatly reduced and sandy slope sediments are formed.

Thus some slopes of the Bahamas and perhaps analogous ancient carbonates may consist of a series of muddy limestones units of alternating authigenic and detrital origin which may be differentiated on the basis of mineralogy and microfabrics.

Stress-Deformation of Carbonate Oozes

Iraj Noorany

The paper presents the results of stress-deformation tests on two deep sea carbonate oozes from the Pacific. The sediment cores were obtained from the equatorial region of the Pacific using a spade corer. The stress-deformation characteristics were measured in triaxial compression and consolidation tests. Various soil moduli were measured under different stress conditions. The long-term compression characteristics of the sediments under sustained stresses were studied by means of very slow consolidation tests with loading periods of several months. The effective stress parameters under slow drained loading conditions were also measured. The results are analyzed and presented in the paper.

Microfabric and Physical Properties of Deep-Sea High Latitude Carbonate Oozes

Frank R. Rack and William R. Bryant

We have evaluated variations in shipboard physical properties (wet-bulk, dry-bulk and grain density, shear strength, porosity, and water content), sediment components, and calcium carbonate and biogenic silica (opal) contents from ODP Sites 689, 690, 747, and 751 through scanning electron microscope (SEM) analysis of sediment microfabric combined with consolidation testing using Anteus back-pressure oedometers and falling-head permeability measurements. These sites record changes in biogenic ooze composition from predominantly carbonate (nannofossil) to siliceous (diatom) ooze during the Neogene in response to the expansion of Antarctic water masses following the opening of Drake Passage. Trends in geotechnical properties reflect changes in depositional and post-depositional processes with time. Analysis of these trends allowed us to study the physical nature of biostratigraphically identified hiatuses and variations in environmental conditions linked to the establishment of a zonal oceanographic circulation pattern across the Antarctic region.

Samples were examined using the SEM both before and after consolidation tests which were step-loaded to pressures of 3200 kPa. The presence of diatoms in these nannofossil oozes strongly influenced the sediment properties and the corresponding microfabric. Siliceous tests are resistant to overburden forces acting upon them and thus the compaction is most evident in the calcareous skeletons. These nannofossil skeletons disassociate into crystallites to close off pore spaces and decrease the permeability of the sediment. The calcareous sediments are typically underconsolidated as determined from preconsolidation pressures from consolidation tests. SEM micrographs from various downhole locations show the state of preservation of the microfossils and their spatial relationships in terms of sedimentary microfabric.

The results of this study address the process of sediment compaction in high-productivity pelagic environments from high-latitude regions and the characteristics of the sedimentary microfabric created by diagenetic processes acting upon these deep-sea deposits.

Permeability Characteristics of Slope and Deep Water Carbonates from a Microfabric Perspective

Dawn Lavoie and William R. Bryant

Permeability, the rate at which fluids move through a porous medium, affects the consolidation and reduction in porosity with time and overburden pressure. The majority of marine clays consist of smectites and illites which are very fine-grained, platey materials. In contrast, carbonate sediments are composed of multi-shaped, multi-sized components. In general, the clay-rich sediments consolidate to lower porosities than carbonates at given overburden pressures and thus, in general, the carbonates are more permeable. This difference is related to microfabric.

Numerous samples recovered from slope to mid-ocean depths were consolidated in the laboratory and permeabilities were determined using falling head permeameters and indirectly by consolidation theory. In these clays, porosity ranged between 75 and 40% and permeability ranged between 1×10^{-6} cm/s to 1×10^{-10} cm/s. In contrast, carbonates with porosities between 60 and 40% had permeabilities which ranged between 1×10^{-4} and 1×10^{-7} cm/s. Samples with varying percentages of carbonate content fall between these two end members. At given porosities, permeabilities within the carbonate samples are determined by microfabric. For example, grain-supported samples have a higher permeability (1×10^{-4} cm/s) than matrix supported samples (1×10^{-6} and 1×10^{-7} cm/s). In general, matrix-supported carbonate samples composed of aragonite needles have higher permeabilities (10^{-5} cm/s) than matrix-supported samples of low-magnesian calcite composed predominantly of coccoliths (1×10^{-6} cm/s). Analysis of Scanning and Transmission Electron micrographs of clays and carbonate sediments confirm the more open microstructure of carbonate sediments as opposed to the more evenly distributed but smaller sized clay micropores.

The Nature of the Ooze-Chalk-Limestone Transition in Marine Carbonates: Evidence from the Ontong-Java Plateau, ODP Leg 130

Roy H. Wilkins, J. Urmos, and Leg 130 Scientific Party

During Leg 130 of the Ocean Drilling Program 5 sites were cored and logged on the top and flanks of the Ontong-Java Plateau, a major physiographic feature of the southwest Pacific Ocean. Of the almost 5 km of sediments recovered, most were marine carbonates composed of between 85% and 99% calcium carbonate. Porosities which were measured aboard the JOIDES Resolution and recorded by downhole logging tools were near 70% at the seafloor and less than 10% at a depth of 1200 meters below the seafloor at the deepest site (ODP Site 807). Corresponding compressional wave velocities increased with depth from near 1.50 km/sec in the near-surface ooze to over 5.0 km/sec in the deep limestones.

We have examined the data in the light of simple rock physics theory. Velocity/porosity systematics for the lowest-velocity sediments are in good agreement with theoretical behavior of unconsolidated mixtures (Wood's Equation). Limestone data fit well the time average equation of Wyllie. The entire data set spans the interval between the two relationships and systematically shifts from Wood to Wyllie with increasing depth. The transition is not totally smooth. A velocity-porosity crossplot reveals distinct subsets of the data. Microfabrics of selected epoxy impregnated samples, viewed using back-scattered electron imaging, are used to document the physical changes in the sediments as they undergo compaction and cementation.

Graphical Modeling as a Tool for Predicting the Microfabric of Cement Aggregates

John A. D. Dickson

The production of two-dimensional images of slices through crystal aggregates can be used to predict the microfabric of calcite cements as observed in planar section. The simplest, archetypal image is generated from a plane, inactive substrate by growth from randomly orientated nuclei of plane-faced rhombohedra. A distal maturation of the fabric occurs through three stages, (a) isolated crystal growth, (b) competitive impingement growth and (c) parallel impingement growth. Wide spacing of crystal nuclei relative to space available for growth prevents full maturation of the fabric leading to granular aggregates. The speed of fabric maturation and its optical properties is influenced by crystallographic form; obtuse forms produce length-slow aggregates, acute forms produce length-fast aggregates and equant forms mature slowest. An active substrate involving epitaxy can cause the second, competitive stage to be eliminated. A change in crystallographic form during growth transforms the fabric.

Plane intercrystalline boundaries between adjacent crystals arise from uniform growth rates, curved boundaries arise from disparate growth rates. The complexity of impinging crystal faces is reflected in the complexity of the intercrystalline boundary. High frequency of enfacial junctions is not generated by impingement growth. Most enfacial junctions in ancient cements are enigmatic.

Graphical models may be utilized to understand complex intracrystalline growth patterns e.g. sectored crystal growth. The stereology of crystal aggregates is greatly assisted by graphical modeling.

Compositional Zoning and Crystal Growth Mechanisms in Carbonates: A New Look at Microfabrics Imaged by Cathodoluminescence Microscopy

Jeanne Paquette, W. Bruce Ward, and Richard J. Reeder

The relationship between composition and growth morphology of calcite remains a central problem in carbonate petrology. Differences in trace-element partitioning occur in synthetic and natural crystals between time-equivalent growth sectors that grew on non-equivalent faces (*sector zoning*), and between time-equivalent portions within single growth sectors (*intrasectoral zoning*). These observations indicate the important influence of surface structure on the growth mechanism and the kinetics of impurity incorporation. Our observations indicate that the geometry and extent of sector (SZ) and intrasectoral (IZ) zoning varies highly with growth rate and crystal habit. The resulting compositional differences, however, are systematically related to the growth morphology. IZ and SZ are common in natural calcite crystals where the wide range of growth forms often results in complex microfabrics which can be imaged by cathodoluminescence (CL). The resulting textures are sometimes misinterpreted as evidence of neomorphism, truncation of growth zones by dissolution or interruption of crystal growth. The recognition of IZ and SZ is therefore essential to a correct interpretation of petrographic fabrics. In addition, since the partitioning of different trace elements between different forms is not uniformly affected by growth rate, we can refine our interpretations of diagenetic conditions by considering data from compositionally heterogeneous cements in the context of their growth habit. Our approach relies mainly on comparisons between CL microfabrics documented in synthetic calcite crystals grown under monitored conditions and those of natural calcite and dolomite cements. This can be extended to some non-luminescent cements where growth microfabrics are revealed by etching.

The similarity of CL microfabrics in natural and synthetic calcites demonstrates the usefulness of growing relatively large, well characterized single crystals as an experimental approach in carbonate geochemistry. A better knowledge of the detailed structure of growth surfaces of carbonate minerals is crucial to a better understanding of their growth mechanisms. The widespread occurrence of IZ and SZ in trace element-bearing calcites also indicates that *effective* partitioning coefficients relevant to natural cements should be determined from synthetic overgrowths large enough to be checked for compositional homogeneity.

Fluid-Inclusion Petrography: A Technique for Determining Diagenetic Environment

Robert H. Goldstein

Fluid inclusions in cements can be studied as microfabrics to discriminate between diagenetic environments. Inclusions trapped near-earth-surface temperature as all liquid, remain all liquid in the lab. Most inclusions trapped as one liquid phase above 40-50°C contract to form a small bubble when cooled to laboratory temperatures. During natural overheating of all-liquid inclusions, internal increase in pressure may result in reequilibration. When cooled to laboratory temperatures, the reequilibration causes small bubbles to nucleate in some originally low-temperature inclusions, and may cause an increase in the gas-to-liquid ratio in some high-temperature inclusions.

Cements precipitated from the vadose zone contain inclusions recording the two-phase nature of the diagenetic system. They are a combination of all gas, all liquid, and two-phase inclusions with highly variable ratios of gas to liquid. Inclusion gases are at one-atmosphere pressure. Natural overheating may cause nucleation of small bubbles in some of the originally all-liquid inclusions.

Cements precipitated in the low-temperature phreatic zone generally contain fluid inclusions that are all liquid. Natural overheating may cause nucleation of small vapor bubbles in some of the originally all-liquid inclusions. Bubble pressures are close to a vacuum.

A growth zone of cement that precipitated in a higher temperature (above about 40-50°C) water-saturated environment will contain inclusions which contain small bubbles with consistent vapor-to-liquid ratio. Natural overheating will cause an increase in vapor-to-liquid ratio for some inclusions and an overall decrease in consistency throughout a population. Bubbles may be near vacuum or under high internal pressure.

Petrographic characteristics of fluid inclusions provide a technique that is useful in identifying cement precipitation from the vadose zone, the low-temperature phreatic zone, or a high-temperature environment, and to identify whether natural overheating has occurred.

The Use of Growth Microfabrics and TEM in Understanding Replacement Processes in Carbonates

W. Bruce Ward and Richard J. Reeder

Most low-temperature carbonates forming from aqueous solutions grow by a layer-spreading mechanism, generally spiral growth at the sites of screw dislocations. Irregularities and heterogeneities in the growth process produce features that provide a record of the growth mechanism, including information on growth directions. These textural growth features include zonations of all types (concentric, sectoral, and intrasectoral), gross morphologies, and many smaller-scale features such as dislocations, modulated structures and fine-scale banding. Most of these growth features have the potential of being *inherited* from a precursor phase by a replacement phase formed as the result of dissolution and precipitation. The exceptions to this are several of the smaller-scale growth features (e.g., dislocations and the modulated structure), many of which are resolvable with transmission electron microscopy. These smaller-scale growth features, which are controlled solely by the growth mechanism, are defined by atomic displacements and have *virtually no chance of being inherited from a precursor mineral.* Those smaller-scale features that provide growth directions, such as growth dislocations, can be contrasted with larger-scale growth features such as zonations, which have the potential of being inherited from a precursor. Thus comparing the orientations of the smaller-scale features with larger-scale growth features can aid in the understanding of replacement processes and in specific cases help determine if growth features in a crystal are either relict or the result of growth of that crystal.

For these features to be useful they need to be pervasive and easily related to other growth features. Only in a few cases have the smaller-scale features been utilized in calcites. **However**, the modulated structure, which is pervasive throughout calcian dolomites, has an orientation parallel to the growth normal, as are growth dislocations; therefore both can be used to document growth directions in relationship to larger-scale growth features. Calcian dolomite rhombs occurring either as cements or as replacements commonly have concentric zonation that is parallel to the gross crystal morphology and the fine-scale banding, and is perpendicular to the modulated structure and growth dislocations. The orientations of the fine-scale growth features are consistent with those of the larger-scale features and are indicative of layered growth of that crystal. Thus, such dolomite rhombs are interpreted to be unmodified. Conversely, if the smaller-scale growth features are found to be inconsistent with the larger-scale features, then this would suggest the possibility of a precursor.

Microfabrics and Compositions in Microcrystalline Limestones

Zakaria Lasemi and Philip A. Sandberg

Cementation-calcitization of metastable lime muds in marine or meteoric waters results in distinct microfabrics and compositions which appear to be related to the dominant precursor mud mineralogy. A microspar fabric (5-18 μm) with pitted neomorphic calcites, which may contain aragonite relic inclusions, characterizes fine-grained limestones which are inferred to have had aragonite-dominated lime mud precursors (ADP micrites). A micrite fabric (2-4 μm) with relic-free, unpitted calcite crystals, on the other hand, is characteristic of fine-grained limestones inferred to have had calcite-dominated lime mud precursors (CDP micrites). Abundance of cement-filled microfenestrae in many micrites (both ADP and CDP micrites) is comparable to that in uncompacted Holocene lime muds, suggesting that cementation-calcitization of the precursor muds occurred early prior to significant burial and, at times, possibly in marine environments. Low-Sr and a positive correlation between Sr and Mg in CDP micrites (compared to high Sr and the negative trend in Sr vs. Mg in ADP micrites) suggest high-Mg calcite dominated lime mud precursors for those CDP micrites. Both ADP and CDP micrites show a relatively uniform temporal distribution, in contrast to the oscillatory trend in mineralogy of inorganic carbonates. This suggests that the precursor lime muds of Phanerozoic micrites were dominantly biogenic.

Microfabrics and Geochemical Trends Associated with Meteoric Alteration of Early, Near-Surface Dolomite

S. L. Dorobek, T. M. Smith, and P. M. Whitsitt

Regional studies of Devonian and Mississippian carbonate sequences in Montana and Idaho illustrate the ability of meteoric water to alter early, near-surface dolomite. Petrographic, stratigraphic, and geochemical evidence suggest that the early dolomites in these rocks formed in various near-surface settings (evaporitic tidal flats, shallow subsurface reflux environments, subtidal marine environments). The best preserved early dolomites, or remnants of them, are nonstoichiometric, isotopically heavy, and trace element enriched. The early dolomites also generally predate compaction fabrics and early calcite cements, and they often exhibit zoned to irregular cathodoluminescence patterns.

However, many of these early dolomites apparently were altered by meteoric fluids in shallow subsurface environments (0-300 m burial depth); meteoric recharge occurred during long-term episodes of subaerial exposure (10^6-10^7 yr). The meteoric alteration includes partial to complete replacement of the early dolomite by later dolomite phases and extensive calcite replacement ("dedolomitization"). Highly altered dolomites occur closest to recharge surfaces and typically are the most stoichiometric, have the most negative $\delta^{18}O$ values, are trace element depleted, and are petrographically homogeneous when observed under cathodoluminescence or back-scattered electron imaging. In some settings, it may be possible to map meteoric flow paths by contouring geochemical data from replacive dolomites. Another geochemical trend which may indicate near-surface alteration of dolomites by meteoric waters is the development of depleted cerium contents ("negative Ce anomaly") in meteoric replacement dolomites. The negative Ce anomaly may develop because Ce^{4+} is preferentially scavenged and incorporated into authigenic Fe-Mn oxyhydroxides in oxidizing near-surface diagenetic environments and therefore is not available for incorporation into the meteoric dolomite.

Retention of original fabrics and geochemical signatures of the early dolomite seems to be most prevalent in downflow regions, far from recharge surfaces. In downflow portions of paleoaquifers, groundwaters most likely were saturated with respect to dolomite because of extensive dissolution of soluble dolomite near recharge areas. Early, pore-filling calcite cements in downflow regions also may seal off porosity, thus preventing reaction of the early, more soluble dolomites with later meteoric waters.

Stylolites, Styloporosity and Stylocement

Alton Brown

Styloporosity and stylocement help document the origin of stylolites and burial cementation history. Three types of porosity along stylolites can be recognized: antecedent, mechanical, and dissolutional. Antecedent styloporosity forms from the intersection of existing pores with stylolites. Antecedent pores can be identified by cements which predate burial. Mechanical styloporosity results from oblique divergence of stylolite surfaces due to change in stress orientation. These pores can be recognized by their smooth walls which conform to precursor stylolite surfaces but crosscut earlier fabric. Dissolutional styloporosity results from dissolution along the stylolite that is unrelated to pressure solution. These pores can be recognized by the lack of early cements and by their irregular walls crosscutting earlier fabric and not conforming to precursor stylolite geometry.

Syndeformational cements are fibrous fracture fills of the syntaxial or stretched-crystal type. The fibers record the change in orientation of the stress during growth and document that precipitation continued as the pore opened. All observed stress orientation changed less than 10 degrees; large changes in stress orientation are represented by a new set of stylolites and no mechanical styloporosity. Post-deformational calcite cements are typical coarse-crystalline blocky spar. Some syndeformational cements may recrystallize to fine- or medium-crystalline blocky calcite due to excessive twinning or strain.

Cements and porosity associated with stylolites are consistent with a pressure-solution mechanism for stylolite formation with rates controlled by stressed-film diffusion at the stylolite. Recently proposed alternate mechanisms for stylolite formation have serious theoretical flaws and are not consistent with the distribution of cements and porosity around stylolites. Mechanical styloporosity is the most common styloporosity type observed in subsurface rocks; however, there is always a net loss of porosity associated with its formation. Dissolutional styloporosity is extremely rare except at outcrops or below major unconformities. In many cases, the styloporosity used as evidence of deep-burial secondary dissolution in limestones appears to be mechanical rather than dissolutional styloporosity. This indicates that deep-burial secondary porosity formation in limestones may be rarer than currently envisioned.

Burial Diagenetic Calcites and Porosity Occlusion

Peter A. Scholle

A number of statistical, petrographic and geochemical arguments have been marshalled in recent years to refine our understanding of burial cements, but none has provided unambiguous results. The most persuasive arguments for the importance of burial-stage calcite cementation come from statistical analysis of porosity distributions in modern and ancient limestones. Petrographic observations on the timing of calcite cement formation relative to unconformities, stylolites, grain breakage, hydrocarbon migration and similar burial-related, and at least somewhat "dateable", events typically provide the strongest direct evidence that a particular cement is of late diagenetic origin. Multi-phase fluid inclusion analyses (homogenization and freezing point studies) hold considerable promise for the determination of cement formation temperatures, although problems with stretching and/or leakage make such data unreliable in many calcites. In this same context, stable isotopic data ($^{13}C/^{12}C$ and $^{18}O/^{16}O$) has proven useful as an adjunct to other tools — the ambiguity between temperature and water chemistry effects, however, typically precludes unequivocal interpretation. Acquisition of trace element (or cathodoluminescence) data, at least on a gross scale, is useful because many late-stage calcites form from relatively stagnant, iron- and manganese-rich pore fluids and thus are enriched in those elements. Finally, analyses of $^{87}Sr/^{86}Sr$, Nd isotopes, and rare earth elements have contributed, in some cases, to an understanding of the environments (especially the paleohydrology) of burial diagenesis.

In very few cases, however, will any one of these tools provide absolute evidence of the time of cement formation. Only through the integration of geochemical tools within a well constrained petrographic and geological (burial history) context can consistent results be achieved. Interestingly, several such modern integrated studies have shown that some calcite cements which were previously thought to have formed during basin burial actually were produced during the uplift phase of basin evolution, although still at considerable depth. This may help to explain the origin of the large volumes of fluids needed to achieve observed geochemical compositions.

Dolomite Crystal Size Distribution in the Burial Environment

D. F. Sibley, J. M. Gregg, R. G. Brown, and P. R. Laudon

Analyses of crystal size distributions were made of natural dolomites from a wide variety of diagenetic environments. The distributions are normal to coarse skewed (log-normal). The variation in skewness within groups from the same environment is as great as between groups. The within group variation is particularly pronounced in epigeneticly dolomitized calcirudites in the Trenton Formation (Ordovician), Michigan. No correlation was found between skewness and mean size, crystal shape, or inferred environment of dolomitization. Variation in crystal size distribution for the mineralized Bonneterre Dolomite (Cambrian), Missouri appears to be controlled by facies. Textural variability of the precursor limestone seems to be the most important factor in determining crystal size distribution in the dolomites studied here.

Crystal size distributions in dolomites place some limits on nucleation and growth models which might apply to dolomitization in all environments. Near normal distributions are consistent with a site saturation model in which all nuclei form at the same time and grow at the same rate until impingement. Coarse skewed distributions are consistent with at least two models: 1) a growth dispersion model in which some crystals grow faster than others, or 2) increasing nucleation rate during dolomitization. Our data requires that different models be applied to samples which are only centimeters apart.

Recrystallization of Dolomite with Time

Julie A. Kupecz

Petrographic, cathodoluminescence, and geochemical (trace element; C, O, and Sr isotopic) data suggest that many ancient dolomites originated as metastable phases, and have undergone multiple episodes of textural and geochemical evolution via neomorphism and mineral stabilization. Because of overprinting by these diagenetic events, geochemical signatures of ancient dolomites must be interpreted in the context of having evolved through time. This has implications for dclomitization studies in interpreting trace element data, and isotopic systems that tend to be fluid-buffered (i.e., del ^{18}O).

The Lower Ordovician Ellenburger Group of west Texas is a classic example of an ancient, thick, widespread, dolomite. The Ellenburger comprises five different generations of dolomite, as defined by standard and cathodoluminescence petrography, which are interpreted to have formed over an extended amount of time (ca. 200 my). Cathodoluminescence and geochemical data document replacement of the earliest (and most volumetrically significant) generation of dolomite by later dolomite generations, and illustrate the progressive evolution of the geochemical signatures. Similar petrographic and geochemical evidence from both modern and ancient dolomites, as documented in the literature, implies that recrystallization of dolomite over time is not uncommon. Therefore, caution in interpreting models for initial dolomitization of ancient dolomitized sequences is suggested. A single model for these types of complex rocks cannot exist.

Genesis of Stylolites and Banded Compaction/Cementation Alternations in Argillaceous Carbonates: A Quantitative Pressure Solution Model

Peter Ortoleva and Thomas Dewers

A quantitative reactional transport/mechanical model of pressure solution is used to explain the development of stylolites and bands of compaction alternating with bands of augmented cementation. These phenomena are shown to be the consequence of an unstable dynamics that takes place during compaction and leads to the intensification of textural contrasts during burial diagenesis. The quantitative model allows for the prediction of the range of existence and properties of these phenomena with variating carbonate grain size, clay content and burial and thermal history variations with changes in pH, p(CO_2) and salinity are also investigated.

The theory is applied to the analysis of marl/limestone alternations. Observed trends with grain size and clay content are explained as is the anti-correlation of clay content and cementation as well as the positive correlation between regions of compaction and highest porosity. Possible effects of Ostwald ripening on the early development of these phenomena are probed.

Effects of Sulfate Reduction on Carbonate Dissolution in Mixing Zone Fluids

Ronald K. Stoessell and William C. Ward

Sulfate reduction in the seawater end-member of mixing zone fluids increases both the acidity and bicarbonate concentrations, shifting the resulting fluid saturation indices for carbonate minerals as a function of percent seawater. Mixing zone fluids were modeled theoretically using Caribbean seawater and a freshwater endmember from Barbados assuming sulfate reduction in the absence and in the presence of goethite.

In the absence of goethite, the calcite saturation indices are shifted towards under-saturation as the percent sulfate reduction approaches 5%. With increasing sulfate reduction, the saturation indices then move towards supersaturation. The fluids are supersaturated throughout the mixing zone composition with greater than 60% sulfate reduction and under-saturated with 1 to 25% sulfate reduction. Sulfate reduction in the presence of goethite shifts the calcite saturation indices towards supersaturation. Fluids containing more than 25% sulfate reduction are supersaturated throughout the range of mixing zone compositions.

Calcite dissolution in fluids with up to 25% sulfate reduction, in the absence of goethite, occurred in the brackish and saline fluids of the mixing zone. Without sulfate reduction the dissolution was less and/or was not predicted in this portion of the mixing zone. The presence of goethite reversed the effect of sulfate reduction, resulting in a decrease in calcite dissolution and/or an increase in calcite precipitation.

In summary, minor amounts of sulfate reduction in the absence of iron minerals significantly enhances the potential for carbonate dissolution in the brackish to saline fluids of the mixing zone. However, similar amounts of sulfate reduction in the presence of iron oxides significantly reduces the potential for carbonate dissolution.

Reinterpretation of Upper Ordovician Red River Carbonates, Cedar Creek Anticline, Williston Basin, USA: Calcrete Weathering of a Shark Bay Ancient Analog

Anna Dombrowski

Red River dolomites produce from subtidal winnowed and burrowed grainstones and also from stromatolitic shallow subtidal/intertidal peloidal grainstones. Macerals recovered from the shoreline grainstones indicated that they were bound by Cloeocapsomorpha prisca Zalessly 1917 which is closely related to the stromatolite-forming cyanobacterium Entophysalis major in modern algal sediments at Shark Bay, Western Australia. Chalky porosity originated from calcrete weathering of very fine grained grainstones with original interparticle porosity. Weathering occurred after incomplete vadose cementation and leaching but prior to dolomite replacement by mixed to normal marine waters. Three shoaling upward cycles and several subcycles each ended with subaerial exposure. Bedded gypsum/anhydrites precipitated from initially restricted waters in each succeeding transgression.

Calcrete weathering features were concentrated immediately below disconformity surfaces and decreased downward. These features included: manganese dioxide dendrites (desert varnish); degrading neomorphism; extensive micrite cement precipitation; cherty-chalky nodules and secondary chalky porosity that cut across depositional features; leaching along microfractures; and organic-rich soil horizons with floatstone breccias. Extensive weathering produced chalky beds 1-3 feet thick, which are highly porous but impermeable with high capillary entry pressures; these are interbedded within the sucrosic reservoir and are distinguishable on wireline logs.

Recognition of calcrete weathering with a diagenetic origin of chalky porosity permitted use of a more realistic depositional model (carbonate ramp with a high-energy grainstone-dominated shoreline) rather than the one previously used (carbonate shelf-slope model with a low-energy mud-dominated shoreline and sabkha). Diagenetic chalky porosity development also explained abrupt variations in reservoir quality that cut across depositional facies.

Classification of Lithified Carbonates Using Ternary Plots of Pore Facies

David C. Kopaska-Merkel and Steven D. Mann

Ternary diagrams whose apices are carbonate pore types (ternary pore plots, or TPPs) are used to graphically summarize quantitative data derived from point counting of thin sections, using a modification of the genetic classification of Choquette and Pray (1970).

TPPs complement engineering data, which give information on the sizes of pore-system elements, whereas thin-section point counting provides information on the shapes and origins of pore-system elements. Thin-section point-count data are cheap and easy to collect, and can be used to guide more-expensive engineering analyses.

TPPs provide insight into a variety of geological problems. (1) The diagenetic processes of dissolution, cementation, and dolomitization play a major role in the evolution of carbonate rock-pore systems. Use of TPPs facilitates recognition of diagenetic processes, gradients, and trends by focusing attention on the distribution of diagenetic products. (2) Pore facies may be recognized by using TPPs. When pore facies are calibrated to other petrophysical information, pore-facies assignment becomes a predictor of other reservoir characteristics, including reservoir performance. (3) TPPs are a powerful tool for evaluating reservoir heterogeneity. Homogeneous reservoirs form tight clusters of points on TPPs; widely scattered points indicate reservoir heterogeneity. Clusters of points from a single well that plot on different parts of a TPP represent flow units: stratigraphic intervals that have significantly different fluid-flow properties.

The use of TPPs is illustrated by a case study of the Smackover Formation in SW Alabama. More than 50 thin sections from five Smackover fields were point counted. Three components account for 95% of pores (moldic plus secondary intraparticle, interparticle, and intercrystalline pores) and form the apices of TPPs.

Cores from lithologically homogeneous reservoirs cluster tightly on TPPs, whereas data points from lithologically heterogeneous reservoirs cluster weakly or not at all. Multiple reservoir lithofacies in one field form discrete clusters on TPPs. Reservoir intervals from different cores may plot close to each other on TPPs, permitting identification of regionally distributed pore facies (e.g., oomoldic dolograinstones from several fields). Poor correlation between porosity and permeability in one field is explainable by differences in pore types recognizable on TPPs.

ABSTRACTS

POSTER PAPERS

Bacterial Bodies and Carbonate Fabrics: Recent to Triassic

Robert L. Folk

Sulfide-rich hot springs in Viterbo, Italy, emerge at over 60°C and rapidly precipitate carbonate, largely aragonite because the temperature is higher than 40°C (as in Yellowstone, Pursell, 1985). Aragonite needles form surface rafts of fuzzy dumbbells, masses of radial spheres as bottom sediment, and "bottle-brushes" around filamentous S-bacteria. Calcite grows later, engulfing aragonite needles, and producing gothic-arch crystals with curving sides and overlapping scales. Under SEM, simple air-dried samples show plump calcified bacteria on the surfaces of these minerals, and on associated mucus sheets and threads. Some bacteria are stable on HCl etching (perhaps because of tough organic cell walls), while others collapse as the carbonate cast is dissolved out of them.

Etching reveals closely-packed swarms of acid-resistant bacteria within many lithified travertine samples. Bacteria are present both as normal-sized individuals (0.5-1 µm-long jelly-bean shapes or spheres), and as minute spheres of about 0.1 µm, probably representing spores, resting, or stressed individuals.

In the Triassic Portoro limestone of Liguria, Italy, we find similar bodies in HCl-etched samples. This microsparite limestone lies at the bottom of a pile of thrust sheets, has been turned upside-down, buried over 5 km, and heated over 200°C. Yet, it contains abundant etch-resistant 0.5-1 µm ellipses and spheres, together with the tiny 0.1 µm resting stages. The similarity in body-appearance between bacteria in Triassic lagoonal limestone and modern hot-spring travertine is striking.

Partial Replacement of Low-Mg Calcite by Low-Mg Calcite: Multi-phase Microfabrics in Blocky Calcite Cements

Vicki A. Pedone and William J. Meyers

Partial replacement of five generations of low-Mg host cement by at least three generations of low-Mg secondary cement occurs throughout a 60 m stratigraphic interval in Givetian bank deposits of the Emanuel Range in the Canning Basin, Western Australia. Some replacement cements are distinguished from host cement by associated microporosity and oxide inclusions, but others are not discernible from host cement in transmitted light. Replacement cements always form in optical continuity with host cement, so that the intricate replacement patterns in these multi-phase fabrics are best detected using cathodoluminescence petrography. The contact between the host and replacement cements is generally non-geometric and smooth, although embayed, corroded contacts are sometimes observed.

Host and replacement cements are chemically distinct. Microprobe analyses of a yellow and non-luminescently banded host cement that is partially replaced by an orange-luminescent calcite reveals that the yellow bands of the host cement have an average of 2700 ppm Mg and 4025 ppm Mn compared to 415 ppm Mg and 1420 ppm Mn in the replacement cement. The host cement has no detectable Fe or Sr, while the replacement cement has an average 1025 ppm Fe and 880 ppm Sr. A single phase sample of banded host cement has an $^{87}Sr/^{86}Sr$ = .71771, with a Sr abundance of 17 ppm. A sample of the mixed banded and orange cement had an $^{87}Sr/^{86}Sr$ = .72011, with a Sr abundance of 440 ppm.

Microporosity, oxides and corroded margins associated with some replacement calcite indicate that some of the fabric resulted from dissolution and secondary cementation. Replacement cement that is indiscernible from the host in transmitted light and lacks corrosive margins may have formed by fine-scale replacement of the host cement. Widespread replacement of low-Mg calcite by low-Mg calcite has not been previously recognized in calcite cements. Recognition of the distinct chemistries of the component phases and the absence of host "memory" effect in spite of the intricate replacement pattern is crucial in sampling and interpreting the geochemistry of the cement.

Unusual Microfabrics and Cements in a Limestone Interbedded with Coal

Carol de Wet and Stephen Moshier

(no abstract)

Fabric Conrols on Microporosity in Skeletons and Matrix in Limestones

Stephen Moshier

(no abstract)

Microbial, Oolitic and Other Microfabrics in 2.5 Billion-Year-Old Platform Dolomite of Western Australia

Bruce M. Simonson and Kathy Schubel

The 2.5 billion year-old Carawine Dolomite of Western Australia contains some of the oldest platform carbonates on earth, yet it displays a diverse and surprisingly well-preserved suite of facies. That microbes played a dominant role in deposition on the Carawine platform is evidenced by an abundance of stromatolites, oncolites, and related wavy lamination formed by trapping and binding of fine carbonate. Strata displaying laminae consisting of nested, concave-up segments with a strong palisade texture are equally abundant; they resemble tufas and may have been formed by carbonate precipitation around coarse cyanobacterial filaments. Subordinant in thickness to and interbedded with these microbial strata are thin layers of oolitic to wave-rippled sand, other grainstones, and flat-pebble conglomerates. Radial and concentric textures are both well-preserved in many of the ooids, and a few oolitic layers coarsen upward to form reverse-graded pisolite layers ca. 10 cm thick which contain both fine geopetal carbonate and fitted fabrics formed by in situ enlargement. The Carawine also contains scattered occurrences of crystal pseudomorphs displaying several different morphologies. These include sprays of silicified prismatic crystals up to 20 cm long ("soda straws"), upward-directed rows of chevron-terminated crystals replaced by carbonate (gypsum pseudomorphs?), and silicified hopper crystals (halite pseudomorphs?). Encrusting the prismatic crystals are thick, botryoidal carbonate cements with an enigmatic zebraic fabric. All of these rocks consist entirely of dolomite, and studies aimed at determining how the various fabrics formed and have been so well preserved since the first half of earth history are still in progress.

Evaporite Replacement Within the Mid-Permian (Leonardian-Guadalupian) Park City Formation, Bighorn Basin, Wyoming

Dana S. Ulmer and Peter A. Scholle

The Park City Formation consists of cyclic subtidal to supratidal carbonates controlled by glacio-eustatic sea level fluctuations and localized tectonic uplift. Subsurface cores show significant preserved interstitial evaporite, but on outcrop this unit has extensive silica and calcite replacement of former gypsum and anhydrite crystals and nodules.

These replacements appear to be a multistage phenomenon. Field and petrographic evidence (matted fabrics in nodules; evaporite inclusions) indicate that silicifacation involved direct replacement of evaporites and probably occurred during early stages of burial. Calcitization, however, appears to be a much later phenomenon and involved precipitation of coarse crystals within evaporite molds. The replacement calcites have a wide range of isotopic values (oxygen -6.04 to -25.02%, average -18.00%; carbon 2.82 to -25.26, average -7.01%; all values relative to PDB). The calcites are typically free of evaporite remnants but are laden with hydrocarbon inclusions.

The light carbon and oxygen isotopic values and the presence of oil inclusions within the calcites support replacement during late diagenesis, generally following hydrocarbon emplacement. The extremely broad isotopic range indicates that calcitization occurred over a long period of time possibly related to thermochemical sulfate reduction and progressive uplift and Tertiary-age hydrologic events. Thus, significant porosity change has taken place in Park City carbonate strata during "late" diagenesis, and the isotopic variations in the calcitized evaporites provide a history of water and hydrocarbon migration through these units.

Microfabrics and Pore-System Development in "Lime-Mud" Shelf Dolomites: Physical Evidence from Limestone-to-Dolomite Transitions

Philip W. Choquette

Sucrosic or *planar-e* dolomites formed by alteration of shallow-marine lime-mud-rich carbonates are widespread in the geologic record. Holocene analogs may be very rare. Reported observations of 0.5-2 µm dolomite rhombs "caught in the act" of directly precipitating in the micropores of some Holocene lime muds seem to suggest that in partly "dolomitized" lime muds pore volume should initially decrease, as Weyl (1960) predicted for other reasons.

In Phanerozoic dolomites, however, pore volume rarely if ever decreases with progressive dolomitization. Rocks from thin (< 1.3 m) limestone-to-dolomite transitions and from other occurrences, interpreted to represent stages of dolomitization, have been analyzed in detail using SEM and CL microscopy and core-analysis methods, and can be modeled using various assumptions. All suites show a progressive increase of % porosity with % "dolomitization". In illustrative suites, with increasing "density" of dolomite rhombs, microvugs appear in the $CaCO_3$ micrite, become more abundant, and evolve into well connected intercrystal pores. Micrite in partially dolomitized rocks commonly has minor amounts of micro-intercrystal pore space. Where $CaCO_3$ allochems then dissolve, their molds may become lined by rhomb-linking overgrowths of dolomite (Choquette, Cox and Meyers, in prep.). Dolomite growth if prolonged should occlude porosity in all-dolomite rocks, and calcite micro-cementation and/or compaction should occlude porosity in partly dolomitized rocks, but in the examples studied neither process has gone to completion. Mass-balance estimates suggest that dolomite-rhomb overgrowth and pore occlusion ended when the supply of $CaCO_3$ on-site was exhausted, implying dolomitization in HCO_3- poor waters. Other diagenetic scenarios would suggest other fabric/porosity models.

Systematic Changes in Texture, Microstructure and Geochemistry of Dolomites During Stepwise Stabilization in the Burial Environment

Isabel P. Montañez

Stratiform replacement dolomites make up to 85% of all dolomite in Early Ordovician, Upper Knox cyclic carbonates. These aphanocrystalline to finely crystalline dolomites formed during tidal-flat progradation associated with high frequency sea-level falls superimposed on third-order sea-level fluctuations. Such near-surface "early" dolomite likely was metastable as is suggested by systematic changes in textures and in microstructures of Knox dolomites that correlate well with trends in trace and major element compositions and stable isotopic signatures. Knox "early" dolomite shows a progressive increase in crystal size with increasing abundance of nonplanar crystal boundaries and zoned overgrowths. Furthermore, more finely crystalline "early" dolomite typically has relict nonluminescent cores with mottled luminescence characteristic of the first generation of burial dolomite. Texturally more mature "early" dolomite lacks relict cores and has homogeneous luminescence similar to that of burial dolomites. Preliminary TEM analysis suggests that these dolomites record a systematic change in microstructures that correlates well with progressive changes in plane-light and cathodoluminescent textures. Knox "early" dolomite shows a trend of decreasing mole % $CaCO_3$ with increasing crystal size and luminescent mottling likely reflecting repeated dissolution-reprecipitation during stabilization. These dolomites also show strong covariant trends between increasing crystal size and decreasing Sr and increasing Mn contents. Covariant trends in the $\delta^{18}O$ values and Sr (moderately so with Mn) contents of Knox early dolomite also record a stabilization history for Knox "early" dolomites. Simultaneous variations in $\delta^{18}O$, Sr and Mn for replacement dolomites were quantitatively modelled (after Banner, 1986) to place constraints on the water-rock interaction history of Knox "early" dolomites. Water-rock models further suggest that Knox "early" dolomites underwent repeated stabilization in shallow to deep burial fluids and that varying degrees of pre-burial geochemical (and textural) signatures are preserved as a function of replacement under varying molar water-rock ratios. Furthermore, burial replacement dolomites in the Knox Group show no covariant trends in trace element or isotopic compositions, nor do they record any systematic changes in textures.

Many modern and ancient near-surface dolomites are initially metastable and are thus susceptible to later diagenetic modification. Stabilization of these dolomites likely occurs in a stepwise manner throughout shallow to deep burial rather than in a single event of recrystallization or neomorphism. Stepwise stabilization of metastable dolomites results in a wide range of textural and geochemical signatures that reflect variable fluid-rock ratios during progressive fluid-rock interaction; much of the initial characteristics of these early dolomites are lost. Consequently, studies that have invoked models of dolomitization for ancient stratiform dolomites based on petrographic and geochemical data have met much resistance. This study demonstrates, however, that a stabilization history and varying degrees of pre-burial geochemical signatures and textures of "early" dolomites commonly are retained in ancient carbonate sequences and can be unravelled by integrating detailed petrographic study with evaluation of covariant textural and geochemical trends and water-rock modelling of such trends.

Microfabric of Travertine-Tufa Carbonates: Examples from Orissa State, India

Manmohan Mohanti and Srikanta Das

Exposures of Quaternary travertine-tufa carbonates in a hilly terrain of Precambrian crystalline rocks have been investigated in parts of Phulbani, Puri and Keonjhar Districts, Orissa State, India. Depositional groups including a complex of carbonates rich in mosses and higher plants, algal crusts, probably microbial/bacterial (?) construction of small cauliflower-like aggregates and spelean-like deposits exhibit a spectra of microfabrics studied in thin sections and by SEM. Algal microfabrics may show laminations and bundles of radial, filamentous structures within calcite spar in a swinging or fan-like disposition and also micrite patches that may be neomorphosed to microspar. SEM observations show calcite thickenings on filaments from 3 µm to 10 µm. Micropores and void spaces exist. Small spherical cauliflower-like aggregates under SEM show smaller roundish to elongated and wavy calcite crystals of 0.3 µm to 1.5 µm extension with interconnected pore system. At places, tapering conical bundles of crystals of average 1.5 µm size occur. Elongated pores may be 5 µm in extension. Thin sections show small isolated rods, roundish to diffuse masses and clumps of darkish opaque spots in calcite microspar suggesting microbial activity. Microbial micrite and microbial spar associations seem likely. Voids in organic-rich travertine-tufas may remain empty or exhibit microfabrics that include uneven fringes of granular calcite cement, gravitational cement and meniscus cement. Thin isopachous cement fringes may be there occasionally. Spelean associations including hard laminated sinter, flowstone, cave grapes and stalactites show a complex of microfabrics in which there are alternations of lighter and darker micritic/microsparry laminae, darkish bands, impurities and thorn-shaped inclusions and some vacuoles. Wedge-shaped, fan-like, bladed/lath-shaped calcite spar, crystals having feathery edges, stubby calcite spar, rhombohedral calcite, 'displasive' calcite spar and radially disposed calcite crystals/crystallites occur as well. Radial crystallites may be cutting across parallel, undulating micritic to microsparry laminae of lighter or darker shades. Crystal sizes and morphology vary widely within the spelean deposits and even in the same level within a crust of few centimetres. Organic (partly microbial) and inorganic processes effecting precipitation and dissolution in a near-surface diagenetic realm of vadose and vadose/phreatic interface are deemed to have controlled the microfabric types.

CONTRIBUTORS

Aharon, Paul
Department of Geology & Geophysics
Louisiana State University
Baton Rouge, Louisiana 70803

Bachman, Richard
Naval Ocean Systems Center
Code 541
San Diego, California 92152-5000
619/553-9862
619/553-3079 - FAX

Bain, Roger J.
Department of Geology
University of Akron
Akron, Ohio 44325
216/972-7659
216/972-6990 - FAX

Bathurst, Robin G. C.
Derwen Dêg Fawr
Llanfair D.C.
Ruthin, Clwyd, WALES
LL15 2SN
44 (0)8245-326

Bennett, Richard H.
Code 360
NOARL
Stennis Space Center, Mississippi 39529
601/688-5460
601/688-4673 - FAX

Boardman, Mark
Department of Geology
Miami University
Oxford, Ohio 45056

Brown, Alton
ARCO Oil & Gas Company
2300 West Plano Parkway
Plano, Texas 75075
214/754-6217
214/754-3691 - FAX

Brown, R. G.
Department of Geological Sciences
Michigan State University
East Lansing, Michigan 48824
517/355-8307

Bryant, William R.
Department of Oceanography
Texas A&M University
College Station, Texas 77843-3146
409/845-2680
409/845-6331 - FAX

Buczynski, Chris
Department of Geosciences
University of Houston
Houston, Texas 77204-5503
713/749-3744
713/747-4527 - FAX

Carney, Cindy K.
Department of Geological Sciences
Wright State University
Dayton, Ohio 45435
513/873-3465
513/873-3301 - FAX

Chafetz, Henry S.
Department of Geosciences
University of Houston
Houston, Texas 77204-5503

Choquette, Philip W.
Department of Geological Sciences
Campus Box 250
University of Colorado at Boulder
Boulder, Colorado 80309-0250
303/492-8141
303/492-2606 - FAX

Das, Srikanta
Department of Geology
Utkal University
Vani Vihar
Bhubaneswar - 751 004 (Orissa)
INDIA

de Wet, Carol B.
Department of Geology
Franklin & Marshall College
Lancaster, Pennsylvania 17604

Dewers, Thomas
Department of Chemistry
Indiana University
Bloomington, Indiana 47405
812/855-2717

Dickson, John A. D. (Tony)
Department of Earth Sciences
University of Cambridge
Downing Street
Cambridge, ENGLAND CB2 3EQ
44 (0)223-333412

Dombrowski, Anna
Shell Western E&P Inc.
P.O. Box 576
Houston, Texas 77001
713/870-2698
713/870-2511 - FAX

Domenico, Patrick A.
Department of Geology
Texas A&M University
College Station, Texas 77843
409/845-0636
409/845-6162 - FAX

Dorobek, Steven
Department of Geology
Texas A&M University
College Station, Texas 77843
409/845-0636
409/845-6162 - FAX

Folk, Robert L.
Department of Geological Sciences
University of Texas at Austin
P.O. Box 7909
Austin, Texas 78713-7909
512/471-5294
512/471-9425 - FAX

Foos, Annabelle
Department of Geology
University of Akron
Akron, Ohio 44325

Goldstein, Robert H.
Department of Geology
120 Lindley Hall
University of Kansas
Lawrence, Kansas 66045-2124
913/864-4974
913/864-7789 - FAX

Gregg, Jay M.
Department of Geology & Geophysics
University of Missouri-Rolla
Rolla, Missouri 65401-0249

Kopaska-Merkel, David C.
Geological Survey of Alabama
P.O. Box 0
Tuscaloosa, Alabama 35486-9780
205/349-2852

Kupecz, Julie A.
ARCO Alaska, Inc.
P.O. Box 100360
Anchorage, Alaska 99510-0360

Lasemi, Zakaria
Department of Geology
245 NHB, 1301 W. Green Street
University of Illinois
Urbana, Illinois 61801
217/333-3541
217/244-4996 - FAX

Laudon, P. R.
Department of Geology & Geophysics
University of Missouri-Rolla
Rolla, Missouri 65401-0249

Lavoie, Dawn L.
Seafloor Geosciences Division
NOARL, Code 361
Stennis Space Center, Mississippi 39529
601/688-4659
601/688-4673 - FAX

Loucks, Robert G.
ARCO Oil & Gas Company
2300 West Plano Parkway
Plano, Texas 75075
214/754-6524
214/754-3692 - FAX

Mann, Steven D.
Geological Survey of Alabama
P.O. Box 0
Tuscaloosa, Alabama 35486-9780
205/349-2852

Meyers, William J.
Department of Earth and Space Sciences
SUNY at Stony Brook
Stony Brook, New York 11794

Mohanti, Manmohan
Department of Geology
Utkal University
Vani Vihar
Bhubaneswar - 751 004 (Orissa)
INDIA

Montañez, Isabel
Department of Earth Sciences
University of California at Riverside
Riverside, California 92521
714/787-3441
714/787-4324 - FAX

Moore, Clyde H.
Department of Geology
Louisiana State University
Baton Rouge, Louisiana 70803
504/388-8224
504/388-6400 - FAX

Moshier, Stephen O.
Department of Geological Sciences
Bowman Hall
University of Kentucky
Lexington, Kentucky 40506-0059
606/257-3932
606/257-4000 - FAX

Neumann, A. Conrad
Marine Sciences Program
5-12 Venable Hall 045A
University of North Carolina
Chapel Hill, North Carolina 27514
909/962-1253
909/962-5604 - FAX

Noorany, Iraj
Civil Engineering Department
College of Engineering
San Diego State University
San Diego, California 92182
619/594-5932
619/594-6005 - FAX

Ortoleva, Peter
Department of Chemistry
Indiana University
Bloomington, Indiana 47405
812/855-2717

Paquette, Jeanne
Department of Earth and Space Sciences
SUNY at Stony Brook
Stony Brook, New York 11794-2100
516/632-8200

Pedone, Vicki A.
Department of Geological Sciences
California State University at Northridge
Monterey Hall, Room 328
18111 Nordhoff Street
Northridge, California 91330
818/885-3541

Rack, Frank
Department of Oceanography
Texas A&M University
College Station, Texas 77843-3146
409/845-2719
409/845-3661 - FAX

Reeder, Richard J.
Department of Earth and Space Sciences
SUNY at Stony Brook
Stony Brook, New York 11794-2100
516/632-8200

Rezak, Richard
Department of Oceanography
Texas A&M University
College Station, Texas 77843-3146
409/845-2155
409/845-6331 - FAX

Roberts, Harry H.
Coastal Studies Institute
Louisiana State University
Baton Rouge, Louisiana 70803
504/388-2395

Sandberg, Philip A.
Department of Geology
245 NHB, 1301 W. Green Street
University of Illinois
Urbana, Illinois 61801
217/333-0228
217/244-4996 - FAX

Scholle, Peter
Department of Geological Sciences
Southern Methodist University
Dallas, Texas 75275
214/692-2750
214/692-4289 - FAX

Schubel, Kathy
Department of Geological Sciences
SUNY at Binghamton
Binghamton, New York 13901

Scoffin, Terence P.
Department of Geology & Geophysics
University of Edinburgh
Grant Institute, West Mains Road
Edinburgh, SCOTLAND EH9 3JW
44 (0)31-667-1081

Sibley, Duncan
Department of Geological Sciences
Michigan State University
East Lansing, Michigan 48824
517/355-8307

Simonson, Bruce M.
Department of Geology
Carnegie Building
Oberlin College
Oberlin, Ohio 44074-1044
216/775-8347
216/775-8886 - FAX

Slowey, Niall
Woods Hole Oceanography Institution
Woods Hole, Massachusetts 02453
508/548-1400
508/548-1400, Ext. 6013 - FAX

Smith, Tad M.
Department of Geology
Texas A&M University
College Station, Texas 77843
409/845-2451

Stoessell, Ronald K.
Department of Geology and Geophysics
University of New Orleans
Lakefront Campus
New Orleans, Louisiana 70148

Tedesco, Lenore P.
University of Miami - RSMAS
Division of Marine Geology & Geophysics
4600 Rickenbacker Causeway
Miami, Florida 33149-1098
305/361-4658
305/361-4632 - FAX

Ulmer, Dana S.
Department of Geological Sciences
Southern Methodist University
Dallas, Texas 75275
214/692-2750
214/692-4289 - FAX

Urmos, J.
Hawaii Institute of Geophysics
2525 Correa Road
Honolulu, Hawaii 96822
808/956-5228
808/956-2538 - FAX

Wanless, Harold R.
University of Miami - RSMAS
Division of Marine Geology & Geophysics
4600 Rickenbacker Causeway
Miami, Florida 33149-1098
305/361-4658
305/361-4632 - FAX

Ward, W. Bruce
Department of Earth and Space Sciences
SUNY at Stony Brook
Stony Brook, New York 11794-2100
516/632-8200
516/632-8240 - FAX

Ward, William C.
Department of Earth Sciences
University of New Orleans
New Orleans, Louisiana 70148

Whitsitt, Philip M.
Department of Geology
Texas A&M University
College Station, Texas 77843
409/845-2451

Wilber, R. Jude
Sea Education Association
Woods Hole, Massachusetts 02453

Wilkens, Roy H.
Hawaii Institute of Geophysics
2525 Correa Road
Honolulu, Hawaii 96822
808/956-5228
808/956-2538 - FAX

MAPS OF LOCAL AREA

BRYAN-COLLEGE STATION, TEXAS

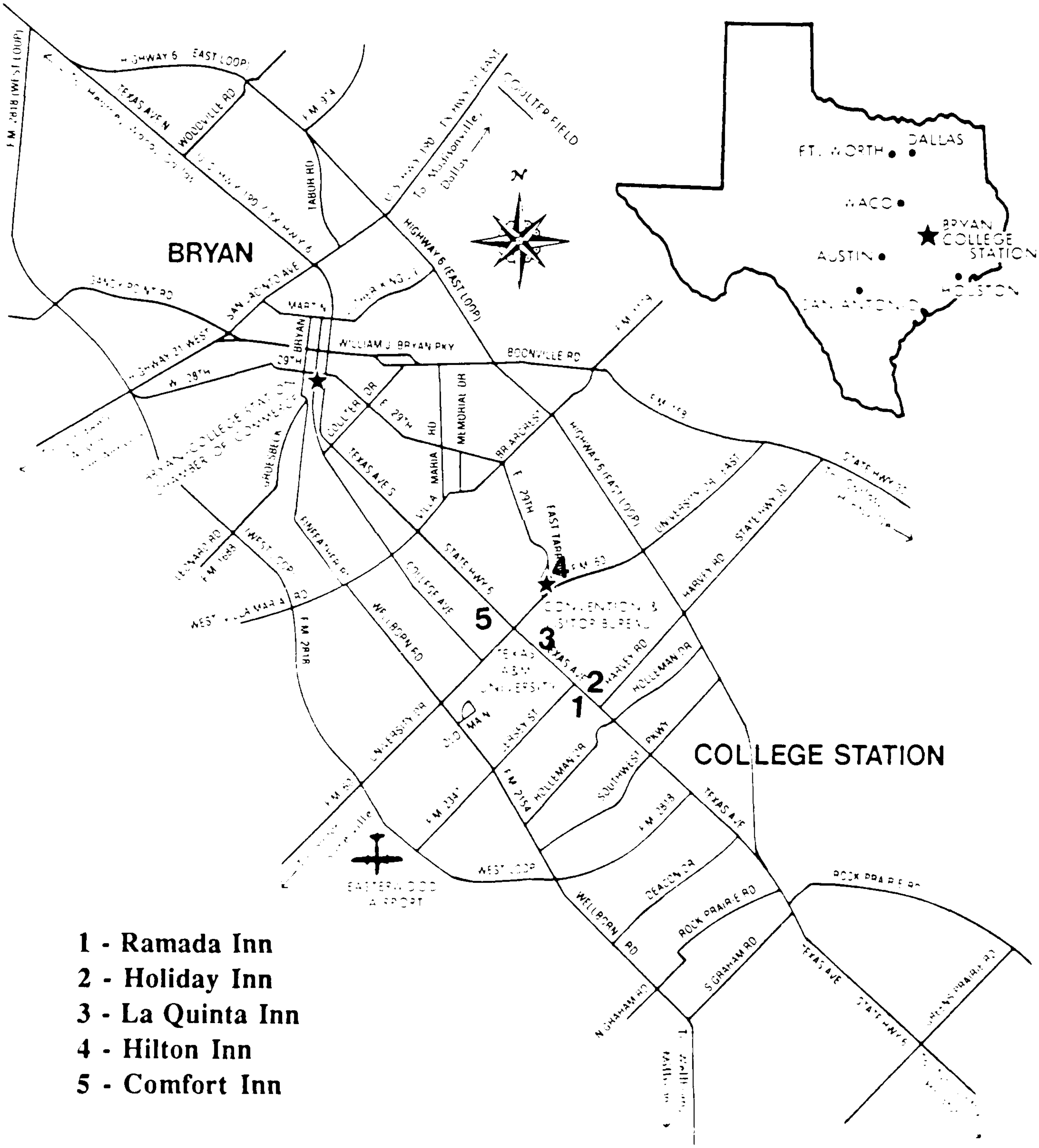

1 - Ramada Inn
2 - Holiday Inn
3 - La Quinta Inn
4 - Hilton Inn
5 - Comfort Inn

TEXAS A&M UNIVERSITY

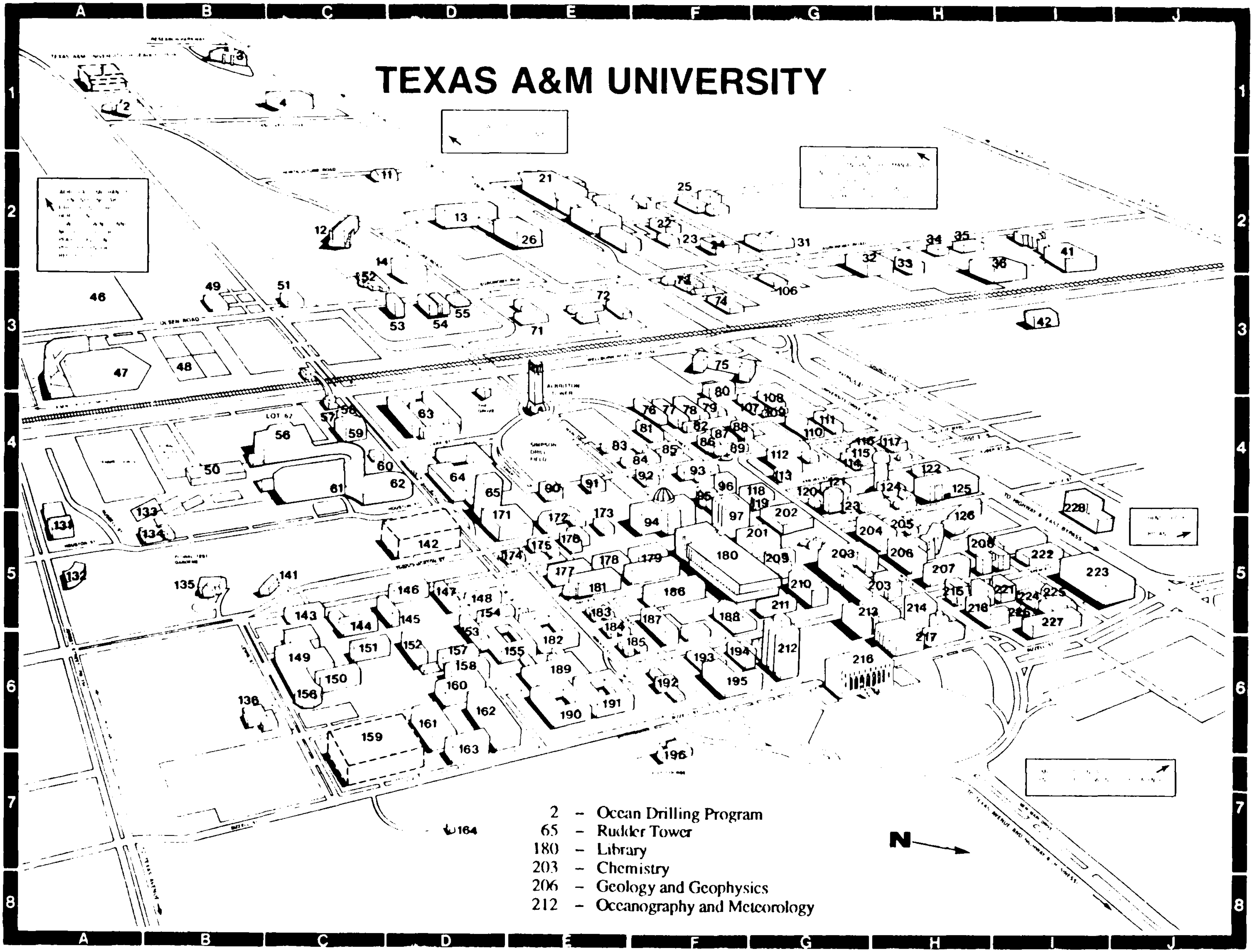

2	–	Ocean Drilling Program
65	–	Rudder Tower
180	–	Library
203	–	Chemistry
206	–	Geology and Geophysics
212	–	Oceanography and Meteorology

NUMERICAL KEY

- [illegible] Offshore Technology Research Center (A 1) (under construction)
- [illegible] Ocean Drilling Program Building [illegible]
- [illegible] Research Park (B 1)
- 4 [illegible] National Training Center [illegible] Meat Inspection School) (C 1)
- [illegible] Advance Lab [illegible]
- [illegible] Horticulture [illegible] Band [illegible]
- [illegible] Reynolds **Medical Sciences** Building (D 2)
- [illegible] Biochemistry Biophysics Building (D 2)
- 21 Veterinary Medical Center (E 2)
- [illegible] Texas Veterinary **Medical** Diagnostic Lab (F 2)
- 23 [illegible] (F 2)
- 24 Laboratory Animal Resources Building [illegible]
- [illegible] Foundation Seed Service [illegible]
- [illegible] **Medical** Sciences Library (E 2)
- 31 Agronomy Field Lab [illegible]
- 32 Purchasing and Stores [illegible]
- 33 Transportation Center [illegible]
- 34 Transportation Annex [illegible]
- 35 Physical Plant Grounds Maintenance Facility (H 2)
- 36 Food Services Commissary [illegible]
- 41 Physical Plant Offices and Shops [illegible]
- 42 Employment Office [illegible]
- 46 Anderson Track and Field Complex Recreational Sports Fields and Golf Driving Range (A 3)
- 4[illegible] Olsen **Baseball** Field (A 3)
- 48 Penberthy **Intramural** Complex (B 3)
- 49 Beef Cattle Center (B [illegible])
- 50 Steed **Research and Conditioning** Laboratory (B 4)
- 51 Utilities Plant Satellite [illegible]
- 52 Rosenthal **Meat Science and Technology** Center (C 3)
- 53 Kleberg **Animal and Food Sciences** Center (D 3)
- 54 Heep Center for **Soil and Crop Sciences and Entomology** (D 3)
- [illegible] Horticulture Greenhouses (D 3)
- 56 Kyle Field (C 4)
- [illegible]
- [illegible]
- [illegible]
- [illegible]
- [illegible]
- 6[illegible] [illegible] **Coliseum** [illegible]
- 6[illegible] [illegible] **Athletic** [illegible]
- 64 [illegible]
- 64 [illegible]
- 65 Holder [illegible]
- [illegible] **Food Protein R&D** Center
- [illegible] Agricultural Engineering [illegible]
- [illegible]
- [illegible]
- [illegible]
- [illegible]
- [illegible]
- [illegible]
- [illegible]
- 80 [illegible] Hall (F 3)
- 81 Henderson Hall (F 4)
- 8[illegible] Hughes Hall (F 4)
- 83 Law Hall [illegible]
- 84 Puryear Hall [illegible]
- 85 All Faiths **Chapel** (F 4)
- 86 McFadden Hall (F 4)
- 87 Hart Hall (F 4)
- 88 Special Services Building (F 4)
- 89 [illegible] Hall (F 4)
- [illegible]
- 91 [illegible] Building (F 4)
- [illegible] YMCA Building (F 4)
- 93 Beutel **Health** Center (F 4)
- 94 Academic Building (F 4)
- 9[illegible] Bolton Hall (F 4)
- 96 Legett Hall (F 4)
- [illegible] Harrington **Education** Center [illegible] (F 4)
- [illegible]
- [illegible]
- [illegible]
- [illegible]
- [illegible]
- [illegible]
- [illegible]
- [illegible]
- [illegible]
- 11[illegible] [illegible]
- [illegible]
- 118 [illegible] (**Engineering Technology**)
- [illegible]
- 121 [illegible] Shop and [illegible] Maintenance Building [illegible]
- [illegible]
- 123 [illegible]
- 124 [illegible] **Mail** [illegible]
- 125 Northside Parking Garage (H 4)
- [illegible]
- [illegible]
- [illegible]
- [illegible] **Tennis** Center [illegible]
- 134 [illegible] (**TV Radio Stations**)
- [illegible] President's Home (B 5)
- 136 [illegible] Building (B 6) (**University Press**)
- 14[illegible] University Officials Home [illegible]
- 142 University Center Parking Garage (D 5) (under construction)
- 14[illegible] [illegible] Residence Hall [illegible]
- 14[illegible] White Hall Residence Hall [illegible]
- 14[illegible] Hart Hall Residence Hall [illegible]
- 146 [illegible] Residence Hall [illegible]
- 14[illegible] [illegible] Residence Hall [illegible]
- 14[illegible] [illegible] Residence Hall [illegible]
- 14[illegible] [illegible]
- [illegible] Residence Hall [illegible]
- [illegible] Residence Hall [illegible]
- [illegible] Residence Hall [illegible]
- 15[illegible] [illegible] Residence Hall [illegible]
- 154 Spence [illegible] Residence Hall [illegible]
- [illegible]
- [illegible] Adams Band Hall (E 6)
- [illegible] Residence Hall 5 (E 6)
- 158 Underwood Hall (D 6)
- 159 Southside Parking Garage (C 6) (under construction)
- 160 Appelt Hall [illegible]
- 161 Eppright Hall (E 6)
- 162 Wells Hall [illegible]
- 163 [illegible] Hall [illegible]
- 164 [illegible] Maintenance Building [illegible]
- [illegible] **Theatre** Complex (E 5)
- 172 Hart Hall [illegible]
- 173 Neeley Hall [illegible]
- 174 [illegible] Satellite (E 5)
- 175 Military Sciences Building (Trigon) (E 5)
- [illegible] Building (E 5)
- [illegible] Building (E 5)
- [illegible] Services Building [illegible]
- [illegible] Sciences Building [illegible]
- 180 [illegible] **Library** [illegible]
- 181 Heldenfels Hall (E 5)
- 18[illegible] [illegible] Hall [illegible]
- 18[illegible] Horticulture Greenhouses (E 5)
- 184 Beasley Lab (E 6)
- 18[illegible] [illegible] Greenhouses [illegible]
- 186 [illegible] Building (F 5) (**Plant Sciences** Building)
- 18[illegible] Dairy Science Building (F 6)
- 188 [illegible] (F 5)
- 189 [illegible]
- 190 Mosher Hall (E 6)
- 191 Krueger Hall (E 6)
- 19[illegible] TAES Annex (E 6)
- 193 Computing Services Center (E 6)
- 194 Animal Industries (E 6)
- 19[illegible] Teague Research Center (E 6)
- 198 Golf Clubhouse [illegible]
- 201 Harrington **Education** Center Classroom (G 5)
- 202 Thompson Hall (G 5)
- 203 Chemistry Building (G 5)
- 204 Reed McDonald Building (H 5)
- 205 Printing Center (H 5)
- 206 Halbouty **Geosciences** Building (H 5)
- 207 Doherty Building (H 5)
- 208 Engineering Physics Building (H 5)
- 209 Francis Hall (G 5)
- 210 Engineering Building (G 5)
- 211 Agriculture Building (G 5)
- 212 Eller **Oceanography and Meteorology** Building (G 6)
- 213 Scoates Hall (G 5)
- 214 Aerospace Engineering Computer Science Building (H 5)
- 215 Richardson **Petroleum Engineering** Building (H 5) (under construction)
- 216 System Administration Building (G 6)
- 217 Langford **Architecture** Center (H 6)
- 218 Civil Engineering Building (H 5)
- 221 CE TTI Building (I 5)
- 222 Cyclotron (I 5)
- 223 Zachry **Engineering** Center (I 5)
- 224 McNew **Engineering Lab** (I 5)
- 225 Hydromechanics Lab (I 5)
- 226 Concrete Materials Lab (I 5)
- 227 Wisenbaker **Engineering Research** Center (I 5)
- 228 Parking Transit and Traffic Services (I 5)

ALPHABETICAL KEY

- 94 Academic Building (F 4)
- 156 Adams Band Hall (E 6)
- 118 Admissions and Records (Heaton Hall) (G 4)
- 11 Advance Lab (C 2)
- 214 Aerospace Engineering Computer Science Building (H 5)
- [illegible] Agricultural Engineering Shops [illegible]
- 211 Agriculture Building (G 5)
- 31 Agronomy Field Lab (G 2)
- 85 All Faiths **Chapel** (F 4)
- 178 Analytical Services Building (E 5)
- 46 Anderson Track and Field Complex (A 3)
- 194 Animal Industries (E 6)
- 160 Appelt Hall (D 6)
- 15[illegible] Aston Hall (E 6)
- 184 Beasley Lab (E 6)
- 4[illegible] Beef Cattle Center (B 3)
- [illegible] Bell Building [illegible]
- 93 Beutel **Health** Center (F 4)
- 13 Biochemistry Biophysics Building (D 2)
- 4 Biological Control Facility [illegible]
- 1[illegible] Biological Sciences Building (E 5)
- [illegible] Bizzell Hall (F 4)
- 12[illegible] Blocker Building (H 4)
- 9[illegible] Bolton Hall (F 4)
- 15[illegible] Briggs Hall Residence Hall 3 (D 5)
- 1[illegible] Butler Building (E 5)
- [illegible] Cain **Athletic** Hall (F 4)
- [illegible] Cater Mattil Hall [illegible] (**Food Protein R&D** Center)
- [illegible] CE TTI Building (I 5)
- 203 Chemistry Building (G 5)
- 218 Civil Engineering Building (H 5)
- [illegible] Clements Hall (F 4)
- 9[illegible] Coke Building (F 4)
- 18[illegible] Commons (E 6)
- 193 Computing Services Center (E 6)
- 226 Concrete Materials Lab (I 5)
- 121 Construction Shop and Grounds Maintenance (G 4)
- 138 Crocker Hall (G 3)
- 222 Cyclotron [illegible]
- 18[illegible] Dairy Science Building (F 6)
- 80 Davis Gary Hall (F 3)
- 59 DeWare Field House (F 4)
- 207 Doherty Building (H 5)
- 58 [illegible] **Natatorium** (F 4)
- 149 Duncan Dining Hall (E 6)
- 182 [illegible] Hall (E 5)
- 212 Eller **Oceanography and Meteorology** Building (G 6)
- 42 Employment Office [illegible]
- 210 Engineering Building (G 5)
- 208 Engineering Physics Building (H 5)
- 120 Engineering Annex (G 4)
- [illegible] Entomology Research Lab [illegible]
- 180 Evans **Library** (F 5)
- 161 Eppright Hall (E 6)
- [illegible] Faculty Building [illegible]
- 11[illegible] Fermier Hall (G 4) (**Engineering Technology**)
- 18[illegible] Floriculture Greenhouse [illegible]
- [illegible] Food Services Commissary [illegible]
- 185 Forestry Greenhouses [illegible]
- 166 Forest Science Lab [illegible]
- [illegible] Foundation Seed Service [illegible]
- 14[illegible] Fountain Hall Residence Hall [illegible]
- [illegible] Fowler Hall (F 4)
- 209 Francis Hall (G 5)
- 4 [illegible] National Training Center [illegible] Meat Inspection School [illegible]
- 15[illegible] Gainer Hall Residence Hall [illegible]
- 1[illegible] Golf Clubhouse [illegible]
- 1[illegible] Golf Course [illegible] Maintenance Building [illegible]
- 46 Golf Driving Range (A [illegible])
- 62 G. Rollie White **Coliseum** (F 4)
- 121 Grounds Maintenance Building (G 4)
- 87 Hart Hall (F 4)
- 206 Halbouty **Geosciences** Building (H 5)
- [illegible]
- 201 Harrington **Education** Center Classroom (G 5)
- [illegible] Harrington **Education** Center Office (F 4)
- [illegible] Harrington [illegible] Residence Hall [illegible]
- 172 Hart Hall [illegible]
- 118 Heaton Hall (G 4) (**Admissions and Records**)
- 54 Heep Center for **Soil and Crop Sciences and Entomology** (D 3)
- 181 Heldenfels Hall (E 5)
- 81 Henderson Hall (F 4)
- 114 Hobby Hall [illegible]
- [illegible]
- [illegible]
- 17[illegible] [illegible] Hall [illegible]
- 8[illegible] Hughes Hall (F 4)
- [illegible]
- [illegible] Kiest Hall [illegible]
- [illegible] Kleberg **Animal and Food Sciences** Center (D 3)
- 1[illegible] Krueger Hall (E 6)
- [illegible] Kyle Field (C 4)
- [illegible] Laboratory Animal Resources Building [illegible]
- [illegible]
- [illegible] Langford **Architecture** Center (H 6)
- 8[illegible] Law Hall (F 4)
- [illegible] Legett Hall (F 4)
- [illegible]
- [illegible] Lechner Hall Residence Hall [illegible]
- 13[illegible] [illegible] Building (B 6) (**University Press**)
- 86 McFadden Hall (F 4)
- 1[illegible] McInnis Hall (G 4)
- 224 McNew **Engineering Lab** (I 5)
- [illegible] **Medical** Sciences Library (E 2)
- 1[illegible] [illegible]
- 175 Military Sciences Building (Trigon) (E 5)
- 11[illegible] Moore Hall (G 4)
- 134 Moore Communications Center (B 5) (**TV Radio Stations**)
- [illegible] Moses Hall (G 4)
- [illegible] Mosher Hall (E 6)
- 190 Mosher Hall (E 6)
- 17[illegible] Neeley Hall (E 5)
- 115 Nocco Hall (G 4)
- 125 Northside Parking Garage (H 4)
- [illegible] Ocean Drilling Program Building (A 1)
- 1 Offshore Technology Research Center (A 1) (under construction)
- 4[illegible] Olsen **Baseball** Field (A 3)
- [illegible]
- 228 Parking Transit and Traffic Services (I 5)
- 18[illegible] [illegible]
- 48 Penberthy **Intramural** Complex (B 3)
- 15[illegible] [illegible] Building (F 5) (**Plant Sciences** Building)
- [illegible] Physical Plant Grounds and Maintenance Facility (H 2)
- 41 Physical Plant Offices and Shops [illegible]
- 11[illegible] [illegible]
- [illegible] President's Home (B 5)
- [illegible] Printing Center (H 5)
- 1[illegible] [illegible]
- [illegible] Purchasing and Stores [illegible]
- 83 [illegible]
- 6[illegible] [illegible]
- 4[illegible] [illegible] Sports Fields [illegible]
- 204 Reed McDonald Building (H 5)
- 18[illegible] [illegible]
- [illegible] Reynolds **Medical Sciences** Building (D 2)
- 215 Richardson **Petroleum Engineering** Building (H 5) (under construction)
- 5[illegible] Rosenthal **Meat Science and Technology** Center (C 3)
- 1[illegible] [illegible]
- 1[illegible] Rudder [illegible] **Theatre** Complex (E 5)
- 6[illegible] Rudder Tower (F 4)
- 11[illegible] Sbisa **Dining** Hall (G 4)
- 111 Schuhmacher Hall (G 4)
- 213 Scoates Hall (G 5)
- 133 Smith **Tennis** Center (B 4)
- 159 Southside Parking Garage (C 6) (under construction)
- 88 Special Services Building (F 4)
- 154 Spence Hall Residence Hall 1 (D 5)
- 50 Steed **Research and Conditioning** Laboratory (B 4)
- 216 System Administration Building (G 6)
- 132 TAES Annex (F 6)
- 195 Teague Research Center (E 6)
- [illegible] Texas Veterinary **Medical** Diagnostic Lab (F 2)
- 202 Thompson Hall (G 5)
- 34 Transportation Annex [illegible]
- 33 Transportation Center (H 2)
- 1[illegible] Twelfth Man Foundation (G 4)
- 158 Underwood Hall (D 6)
- 64 [illegible] 171 University Center (F 4, E 5)
- 142 University Center Parking Garage (D 5) (under construction)
- 124 University **Mail** Service (H 4)
- 141 University Officials Home (C 5)
- 131 University Police (A 5)
- 14[illegible] [illegible] Hall Residence Hall 12 (C 5)
- 1[illegible] Utilities Plant [illegible]
- [illegible] Utilities Plant Satellite [illegible]
- 1[illegible] Utilities Plant Satellite (E 5)
- 21 Veterinary Medical Center (E 2)
- [illegible]
- 1[illegible] Walton Hall (G 4)
- 1[illegible] Wells Hall (E 6)
- 144 White Hall Residence Hall [illegible]
- 15[illegible] Whiteley Hall Residence Hall [illegible]
- 1[illegible] [illegible] Williams [illegible] Alumni Center [illegible]
- 227 Wisenbaker **Engineering Research** Center (I 5)
- [illegible] Wofford [illegible] Pool (F 4)
- 9[illegible] YMCA Building (F 4)
- 223 Zachry **Engineering** Center (I 5)

EIS 89 181 9.88

REPORT DOCUMENTATION PAGE

Form Approved
OBM No. 0704-0188

Public reporting burden for this collection of information is estimated to average 1 hour per response, including the time for reviewing instructions, searching existing data sources, gathering and maintaining the data needed, and completing and reviewing the collection of information. Send comments regarding this burden or any other aspect of this collection of information, including suggestions for reducing this burden, to Washington Headquarters Services, Directorate for information Operations and Reports, 1215 Jefferson Davis Highway, Suite 1204, Arlington, VA 22202-4302, and to the Office of Management and Budget, Paperwork Reduction Project (0704-0188), Washington, DC 20503.

1. Agency Use Only *(Leave blank).*

2. Report Date.
September 1990

3. Report Type and Dates Covered.
Final

4. Title and Subtitle.
Carbonate Microfabrics Symposium and Workshop
September 30 - October 3, 1990

5. Funding Numbers.

Program Element No.	61153N
Project No.	03207
Task No	330
Accession No.	DN255014

6. Author(s).
D. L. Lavoie

7. Performing Organization Names(s) and Address(es).
Naval Oceanographic and Atmospheric Research Laboratory
Ocean Science Directorate
Stennis Space Center, Mississippi 39529-5004

8. Performing Organization Report Number.
SP 060:361:90

9. Sponsoring/Monitoring Agency Name(s) and Address(es).
Naval Oceanographic and Atmospheric Research Laboratory
Basic Research Management Office
Stennis Space Center, Mississippi 39529-5004

10. Sponsoring/Monitoring Agency Report Number.
SP 060:361:90

11. Supplementary Notes.
Co-sponsored by Texas A&M University
College Station, Texas 77843

12a. Distribution/Availability Statement.
Approved for public release; distribution is unlimited.

12b. Distribution Code.

13. Abstract *(Maximum 200 words).*

Abstracts from 27 oral papers and 9 poster papers presented at the Carbonate Microfabrics Symposium and Workshop September 30 - October 3, 1990.

14. Subject Terms.
(U) Geoacoustics, (U) Penetration, (U) Penetrometers, (U) Geotechnical Properties
(U) Sedimentology, (U) Permeability

15. Number of Pages.
60

16. Price Code.

17. Security Classification of Report.	18. Security Classification of This Page.	19. Security Classification of Abstract.	20. Limitation of Abstract.
Unclassified	Unclassified	Unclassified	SAR

NSN 7540-01-280-5500

Standard Form 298 (Rev. 2-89)
Prescribed by ANSI Std. Z39-18
298-102